Stoichiometric and Catalytic Reactions of the Polysiloxane-Bound (Ether–phosphine)rhodium(I) Complex [ClRh($\overset{\frown}{PO}$)(P ~ O)] in Interphases**

Ekkehard Lindner,* Theodor Schneller, Friedrich Auer,
Peter Wegner, and Hermann A. Mayer

Dedicated to Professor H. D. Kaesz on the occasion of his 65th birthday

Abstract: The reaction of four equivalents of the monomeric trimethoxysilyl(T)-functionalized ether–phosphine ligand $CyP(CH_2CH_2OCH_3)(CH_2)_3SiR_3$ (R = OMe [**1a(T^0)**], Me [**1b**]) with [{μ-ClRh(COE)$_2$}$_2$] yielded the monomeric pseudo 14 electron rhodium(I) complexes [ClRh($\overset{\frown}{PO}$)(P ~ O)] (**2a(T^0)$_2$**, **2b**). For the sol–gel process the complex **2a(T^0)$_2$** was protected by introduction of the volatile, reversibly binding ligand pyridine. Thus, the monomeric compound **2a(T^0)$_2$** was co-condensed with two and eight equivalents of the co-condensation agent $MeSi(OMe)_2(CH_2)_6(MeO)_2SiMe$ (**D^0-C_6-D^0**) to give the polysiloxane-bound congeners **2(T^n)$_2$(D^i-C_6-D^i)$_y$** ($y = 2$ and 8, respectively; $i = 0-2$; $n = 0-3$). The polysiloxane-bound complex **2(T^n)$_2$(D^i-C_6-D^i)$_2$** was treated with a variety of small molecules in the gas/solid and liquid/solid interphases. It was shown that a facile cleavage of the Rh–O bond in the ether–phosphine chelate occurred even in the solid state. The reaction of **2(T^n)$_2$(D^i-C_6-D^i)$_2$** with carbon monoxide, carbon disulfide, and diphenylacetylene resulted in the irreversible coordination of the molecule to the metal. In the presence of pyridine, the polysiloxane-bound complex **2(T^n)$_2$(D^i-C_6-D^i)$_2$** oxidatively added hydrogen to give the octahedrally configurated complex [$ClRhH_2(Py)(P\sim O)_2$] [**6(T^n)$_2$(D^i-C_6-D^i)$_2$**]. Treatment of dry **2(T^n)$_2$(D^i-C_6-D^i)$_2$** with ethene led to the reversible formation of the corresponding complex. Although the materials display low surface areas, at least 75% of the rhodium centers within the matrix are accessible to the rather bulky tolan molecules. The complexes **2(T^n)$_2$(D^i-C_6-D^i)$_y$** ($y = 2$, 8) show high activities and selectivities in the hydrogenation of tolan. The conversion was found to depend markedly on the amount of co-condensate **D^0-C_6-D^0** and on the polarity of the solvent. The polysiloxane-bound complexes **2(T^n)$_2$(D^i-C_6-D^i)$_y$** are more active than their monomeric congener **2a(T^0)$_2$**.

Keywords
immobilized catalysts · polysiloxanes · P ligands · rhodium · sol–gel processes

Introduction

Chemical systems in which the reactive centers are anchored to polymeric matrices are gaining in significance because they are able to combine the advantages of both homogeneous and heterogeneous catalysts.[1, 2] In this context sol–gel chemistry opens up the prospect of preparing suitable polymer frameworks under mild and low-temperature conditions.[3–8] The simultaneous co-condensation of trimethoxysilyl(T)-functionalized transition metal complexes with Q, T, D, or D-C_z-D alkoxysilanes [$Q^0 = Si(OEt)_4$; $T^0 = MeSi(OMe)_3$; $D^0 = Me_2Si(OEt)_2$; D^0-C_z-D^0 = $MeSi(OMe)_2(CH_2)_z(MeO)_2SiMe$, $z = 6, 8, 14$] allows these materials to be modified extensively (Figure 1). The resulting Fn–T/Q, Fn–T/T, Fn–T/D, and Fn–T/D-C_z-D blends[9] are organometallic–inorganic hybrid materials, which can be formed with a wide variety of anchored metal complexes and excellent properties; for example, 1) the density of functional groups can be adjusted, 2) the leaching of the catalysts reduced, and 3) a high degree of condensation achieved.[4, 10] Even sensitive metal complexes can be processed by sol–gel methods provided that a special "trapping" technique is applied. This was recently demonstrated with the polycondensation of a water-labile (ether–phosphine)palladium(II) complex.[11] These polymer networks are considered to be stationary phases consisting of the matrix (polysiloxane), the spacer ($-CH_2-CH_2-$), and the reactive center (metal complex).[12] They can overcome the problems encountered with the surface coverage in silica gel,[13–15] such as leaching of functional groups and the restricted loading of catalysts. Appropriate

---

[*] E. Lindner, T. Schneller, F. Auer, P. Wegner H. A. Mayer
Institut für Anorganische Chemie, Universität Tübingen
Auf der Morgenstelle 18, D-72076 Tübingen (Germany)
e-mail: hermann.mayer@uni-tuebingen.de

[**] Supported Organometallic Complexes Part 14. Part 13: E. Lindner, A. Jäger, F. Auer, W. Wielandt, P. Wegner, *J. Mol. Catal.* in press.

Notation used in this paper: Fn = functionality; D, T, and Q denote alkoxysilanes with two, three, and four Si–O bonds, respectively; the superscript denotes the number of Si-O-Si bonds formed during the sol–gel process and is a measure of cross-linkage; for example, $T^0 = MeSi(OMe)_3$. P ~ O: η^1-P-coordinated ether–phosphine ligand; $\overset{\frown}{PO}$: η^2-O,P-chelating ether–phosphine ligand. Cy = cyclohexyl, COE = cyclooctene, Py = pyridine.

0947-6539/97/0311-1833 $ 17.50+.50/0

gaseous or liquid reactants (mobile phases) are able to penetrate these stationary phases on a molecular scale forming interphases, that is, homogeneous mixtures are not formed (see Figure 1).

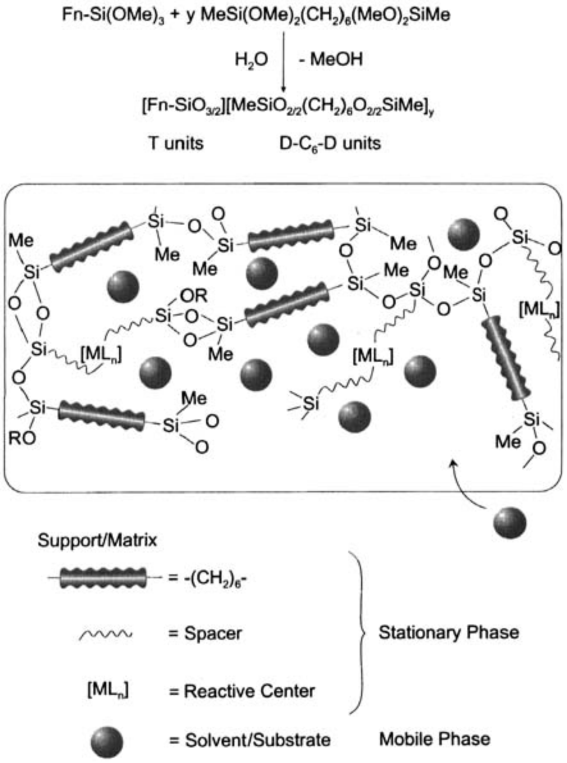

Figure 1. Schematic description of an interphase.

In the interphases the active centers become highly mobile simulating the properties of a solution, and a fast exchange process in the ligand sphere of a transition metal complex can even occur. A good example of these properties is the fluxional behavior of the polysiloxane-bound nonrigid complex $[HRuCl(P\sim O)_2(\overset{\frown}{PO})]$ in the interphase.[12] It has been demonstrated that all three ether–phosphine ligands compete for one coordination site. The fluxionality of the system is a precondition for the catalytic activity of a complex. However, the activities and selectivities of various types of anchored organometallic catalysts are still not satisfactory.

In recent investigations we examined the dynamic properties of the T-functionalized ether–phosphine ligands $PhP(CH_2CH_2OCH_3)(CH_2)_xSi(OMe)_3$ ($x = 3, 6, 8$) and their ruthenium, palladium, and rhodium complexes, which were bound to a variety of silicon matrices.[10, 16, 17] Different mobilities were found depending on the nature of the co-condensate and the length of the spacer ($Fn-T/Q \ll Fn-T/T < Fn-T/D\text{-}C_6\text{-}D \approx Fn-T/D\text{-}C_8\text{-}D < Fn-T/D\text{-}C_{14}\text{-}D < Fn-T/D$; $x = 3 < 6 < 8$).[9] The bis(silylated) network modifiers $\mathbf{D^0\text{-}C_z\text{-}D^0}$ form highly cross-linked polymer frameworks, but still show high mobilities. In contrast to the Fn–T/D copolymers, the metal complex density within the $Fn-T/D\text{-}C_6\text{-}D$ systems can be tuned. It is expected that high mobility combined with sufficient swelling ability of the stationary phases would lead to more uniform reactive centers and therefore to better accessibility, turnover frequency, and selectivity in the catalytic and stoichiometric interphase reactions.

In continuation of this work, we set out to examine the possibility of embedding the catalytically active (ether–phosphine)rhodium(I) complex of the type $[ClRh(\overset{\frown}{PO})(P\sim O)]$ in a polysiloxane network. In the design of this stationary phase the co-condensation agent $\mathbf{D^0\text{-}C_6\text{-}D^0}$ was employed in the sol–gel process, owing to its above-mentioned favorable properties. An important objective of the present work is the investigation of the accessibility of the transition metal center within the stationary phase. Therefore, stoichiometric and catalytic model reactions have been performed at the reactive center in gaseous/solid and liquid/solid interphases. The opening of the $\eta^2\text{-}\overset{\frown}{PO}$ chelate by the coordination of various substrate molecules and the oxidative addition of hydrogen under mild conditions were selected as stoichiometric reactions. In addition, the catalytic activities and selectivities of the polysiloxane-bound rhodium(I) complex $\mathbf{2(T^n)_2(D^i\text{-}C_6\text{-}D^i)_y}$[18] (Scheme 4) in the hydrogenation of diphenylacetylene (tolan) has been studied.

The stereochemistry of the transition metal complexes is established by IR, ^{31}P, and ^{13}C CP/MAS solid state NMR spectroscopy. For the determination of the degree of condensation of the matrix components and the integrity of the hydrocarbon backbone of the ligand and the co-condensate, ^{29}Si and ^{13}C CP/MAS NMR spectroscopy are applied.

Results and Discussion

Synthesis and Characterization of the Monomeric Ligands and Complexes: The reaction of the starting compound $[\{\mu\text{-}ClRh(COE)_2\}_2]$ with four equivalents of the O,P ligand $PhP(CH_2CH_2OCH_3)(CH_2)_3Si(OMe)_3$ in acetone resulted in the formation of a mixture of the neutral monochelate complex $[ClRh(\overset{\frown}{PO})(P\sim O)]$ and the dimeric species $[\{\mu\text{-}ClRh(P\sim O)_2\}_2]$. Cleavage of the chloro bridges under UV irradiation, as described earlier,[19] led to a decomposition of the complexes. The more basic ether–phosphine ligands $\mathbf{1a(T^0)}$ and $\mathbf{1b}$ were therefore prepared (Scheme 1). The intermediate cyclohexyl(methoxyethyl)phosphine was obtained by treatment of the cor-

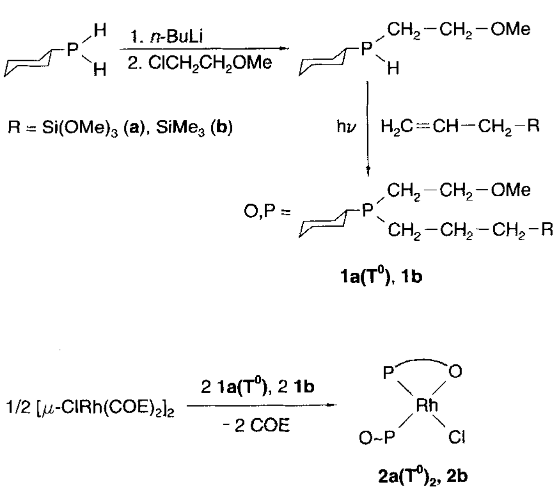

Scheme 1. Synthesis of the monomeric ether–phosphine ligands $\mathbf{1a(T^0)}$ and $\mathbf{1b}$ and of their monochelated rhodium(I) complexes $\mathbf{2a(T^0)_2}$ and $\mathbf{2b}$.

responding lithium phosphide HP(Cy)Li with 1,2-chloromethoxyethane in THF.[20] Photochemically induced addition of the secondary phosphine $HP(Cy)(CH_2CH_2OCH_3)$ to the olefinic double bond of the allylsilanes $CH_2{=}CHCH_2SiR_3$ [R = OMe (**a**), Me (**b**)] gave the ether–phosphine ligands **1a**(**T⁰**) and **1b**, respectively, in high yields.[21] This method was found to be generally applicable for the preparation of a variety of silylalkyl(ether)phosphines.[22] These ether–phosphines contain a strong phosphorus donor atom and an oxygen functionality incorporated in an open chain or in a cyclic ether moiety, which is able to stabilize coordinatively unsaturated metal complexes by formation of a weak metal–oxygen bond.[23] In addition, **1a**(**T⁰**) contains a hydrolyzable trimethoxysilyl group, whereas **1b** has a nonhydrolyzable trimethylsilyl group and can thus be used in model reactions under sol–gel conditions (see below).

Treatment of a suspension of $[\{\mu\text{-ClRh(COE)}_2\}_2]$ in acetone with the ligands **1a**(**T⁰**) and **1b** led to the quantitative formation of the monomers $\mathbf{2a(T^0)_2}$ and **2b**, respectively, as orange oils (Scheme 1), which are analogues of the Wilkinson complex.[24, 25] The products are rather air sensitive and decompose slowly even when stored under an inert atmosphere. At low temperatures (243 K in C_6D_6) the $^{31}P\{^1H\}$ NMR spectrum of $\mathbf{2a(T^0)_2}$ displays two well-resolved AB parts of two ABX systems for the two different phosphine ligands [two diastereomers, due to the chirality of **1a**(**T⁰**)]. For the assignment of these diastereomers a two-dimensional $^{31}P,^{31}P\{^1H\}$ COSY NMR spectrum was recorded. The chemical shifts and coupling constants of $\mathbf{2a(T^0)_2}$ agree well with those of similar known complexes.[24, 25] The values of the $^2J(PP)$ coupling constants (Table 2) are consistent with the *cis* arrangement of the phosphine ligands as displayed in Scheme 1. Owing to its incorporation into a five-membered ring, the phosphorus atom of the chelated ligand resonates at lower field.[26, 27] This is also reflected in the $^{13}C\{^1H\}$ NMR spectrum of $\mathbf{2a(T^0)_2}$ in which the signals of the OCH_2 and OCH_3 groups of the η^2-($\widehat{PO}$)-coordinated ether–phosphine ligand are shifted to lower field. These resonances are observed as multiplets (diastereomers). The FD mass spectrum of $\mathbf{2a(T^0)_2}$ confirms its composition. The model compound **2b** (Scheme 1) shows nearly the same chemical shifts and coupling constants as $\mathbf{2a(T^0)_2}$ in its $^{31}P\{^1H\}$ NMR spectrum (see Experimental Section).

The monomeric (ether–phosphine)rhodium(I) complexes $\mathbf{4a(T^0)_2}$–$\mathbf{8a(T^0)_2}$ (Scheme 2) were synthesized from $\mathbf{2a(T^0)_2}$ by analogy to the reactions of $[ClRh(\widehat{PO})(P{\sim}O)]$ [O,P = $Cy_2P(CH_2CH_2OCH_3)$] with CO, CS_2, H_2/pyridine, ethene, and diphenylacetylene (see Experimental Section).[25, 28] The complexes $\mathbf{4a(T^0)_2}$–$\mathbf{6a(T^0)_2}$ and $\mathbf{8a(T^0)_2}$ were fully characterized by $^{31}P\{^1H\}$ NMR, $^{13}C\{^1H\}$ NMR, ^1H NMR, and IR spectroscopy, and by mass spectrometry (see Experimental Section).[29] The data obtained are in good agreement with those of analogous complexes and confirm the geometries of the compounds shown in Scheme 2.[25, 28] In the case of the CS_2 adduct $\mathbf{5a(T^0)_2}$ the $^{31}P\{^1H\}$ NMR spectrum reveals four doublets with nearly identical $^1J(RhP)$ coupling constants (Experimental Section), which are attributed to four diastereomers. If the two chiral phosphine ligands are taken into account, only two diastereomers are expected. The four diastereomeric forms are explained by the nonplanar $Rh{-}CS_2$ fragment containing an η^2-(C,S)-coordinated carbon disulfide, which leads to an additional center of chirality at the carbon atom of the CS_2 fragment.[28, 30] Although $\mathbf{2a(T^0)_2}$ is closely related to the above-mentioned complex $[ClRh(\widehat{PO})(P{\sim}O)]$ with the ligand $Cy_2P(CH_2CH_2OCH_3)$, its reactivity toward ethene, hydrogen, and oxygen is rather different. When oxygen was bubbled through a solution of $\mathbf{2a(T^0)_2}$ at 233 K, the corresponding dioxygen complex $[ClRhO_2(\widehat{PO})\text{-}(P{\sim}O)]$ was not formed, and the ether–phosphine ligand was quantitatively oxidized. In contrast to $[ClRh(C_2H_4)(P{\sim}O)_2]$ [O,P = $Cy_2P(CH_2CH_2OCH_3)$], the η^2-ethene complex $\mathbf{7a(T^0)_2}$ was only found to be stable in the presence of ethene. Under vacuum $\mathbf{7a(T^0)_2}$ extruded ethene, and the monochelated complex $\mathbf{2a(T^0)_2}$ was regenerated. The $^{31}P\{^1H\}$, $^{13}C\{^1H\}$, and ^1H NMR data compare well with those of other η^2-ethene rhodium(I) complexes.[24, 28]

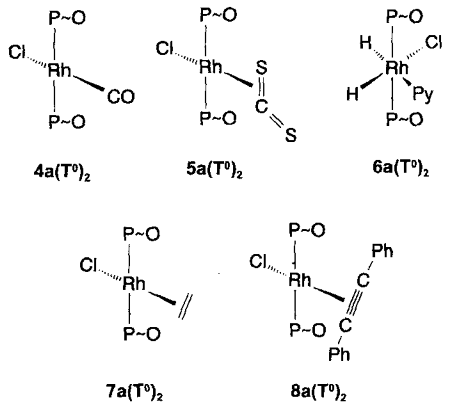

Scheme 2. Products from the reaction of the monomeric chelated rhodium(I) complex $\mathbf{2a(T^0)_2}$ with CO, CS_2, H_2/Py, C_2H_4, and tolan.

Treatment of a solution of $\mathbf{2a(T^0)_2}$ in [D$_8$]toluene with hydrogen (1 bar) at ambient temperature led to an oxidative addition of H_2 (Scheme 3). This reaction is completely reversible. The $^{31}P\{^1H\}$ NMR spectrum displays two groups of doublets in a ratio of 1:1. Three diastereomeric forms can be distinguished in this spectrum. The $^1J(RhP)$ coupling constants of the low-field doublets are typical for a square-planar geometry of binuclear rhodium(I) complexes of the type $[\{\mu\text{-ClRh(PR}_3)_2\}_2]$, while the group of resonances at about $\delta = 28$ reveal $^1J(RhP)$ coupling constants characteristic for octahedral rhodium(III) complexes (see Experimental Section). Only the phosphorus nuclei that resonate at higher field interact with the hydride protons. In the hydride region of the ^1H NMR spectrum of $\mathbf{9a(T^0)_4}$ the typical A_2 part of an A_2M_2X spin system is observed. These data sets are in agreement with those obtained for the binuclear mixed-valent Rh^{III}/Rh^{I} complex $[H_2Rh(PPh_3)_2(\mu\text{-Cl})_2Rh(PPh_3)_2]$ and corroborate the generation of the corresponding dihydride product $\mathbf{9a(T^0)_4}$ (Scheme 3).[31, 32]

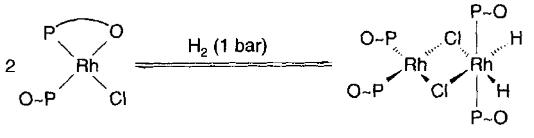

Scheme 3. Reaction of $\mathbf{2a(T^0)_2}$ with hydrogen.

Preparation of the Polycondensed Mono(chelate)rhodium(I) Complexes (see Table 1): The hydrolysis and polycondensation of a mixture of the monomeric rhodium complex $\mathbf{2a(T^0)_2}$ with the co-condensation agent $\mathbf{D^0{-}C_z{-}D^0}$, water, and EtOH, in the presence of any one of the catalysts $(n\mathrm{Bu})_2\mathrm{Sn(OAc)}_2$, NaOH, $\mathrm{NEt_3}$, HCl, or $\mathrm{NH_4F}$ led to the decomposition of the metal complex. The polycondensation catalysts are responsible for this result. We were therefore interested in finding out whether it might be possible to stabilize the labile transition metal complex $\mathbf{2a(T^0)_2}$ during the polycondensation process by introducing a volatile ligand that binds reversibly. When the latter is eliminated by evaporation after the sol–gel transition, the desired complex should be generated within the matrix.[11] Pyridine was found to easily cleave the Rh–O bond and to coordinate reversibly to $\mathbf{2a(T^0)_2}$ and **2b** forming the *cis/trans* isomers of $[\mathrm{ClRh(Py)}(P\sim O)_2]$ [$\mathbf{3a(T^0)_2}$, **3b**; Scheme 4].

Table 1. Copolymers prepared and the corresponding monomers.[18]

Monomeric complex		*y* [a]	Product
$[\mathrm{ClRh}(\overset{\frown}{PO})(P\sim O)]$	$[\mathbf{2a(T^0)_2}]$	2	$\mathbf{2(T^n)_2(D^i{-}C_6{-}D^i)_2}$
		8	$\mathbf{2(T^n)_2(D^i{-}C_6{-}D^i)_8}$
$[\mathrm{ClRh(Py)}(P\sim O)_2]$	$[\mathbf{3a(T^0)_2}]$		
$[\mathrm{ClRh(CO)}(P\sim O)_2]$	$[\mathbf{4a(T^0)_2}]$	2	$\mathbf{4(T^n)_2(D^i{-}C_6{-}D^i)_2}$
$[\mathrm{ClRh(CS_2)}(P\sim O)_2]$	$[\mathbf{5a(T^0)_2}]$	2	$\mathbf{5(T^n)_2(D^i{-}C_6{-}D^i)_2}$
$[\mathrm{ClRhH_2(Py)}(P\sim O)_2]$	$[\mathbf{6a(T^0)_2}]$	2	$\mathbf{6(T^n)_2(D^i{-}C_6{-}D^i)_2}$
$[\mathrm{ClRh(C_2H_4)}(P\sim O)_2]$	$[\mathbf{7a(T^0)_2}]$	2	$\mathbf{7(T^n)_2(D^i{-}C_6{-}D^i)_2}$
$[\mathrm{ClRh(PhC{\equiv}CPh)}(P\sim O)_2]$	$[\mathbf{8a(T^0)_2}]$	2	$\mathbf{8(T^n)_2(D^i{-}C_6{-}D^i)_2}$
$[\mathrm{H_2Rh}(P\sim O)_2(\mu\text{-Cl})_2\mathrm{Rh}(P\sim O)_2]$	$[\mathbf{9a(T^0)_4}]$	2	[b]

[a] Amount *y* of the co-condensation agent $\mathrm{D^0{-}C_6{-}D^0}$. [b] The oxidative addition of $\mathrm{H_2}$ to $\mathbf{2(T^n)_2(D^i{-}C_6{-}D^i)_2}$ gives at least two compounds, which cannot be satisfactorily characterized.

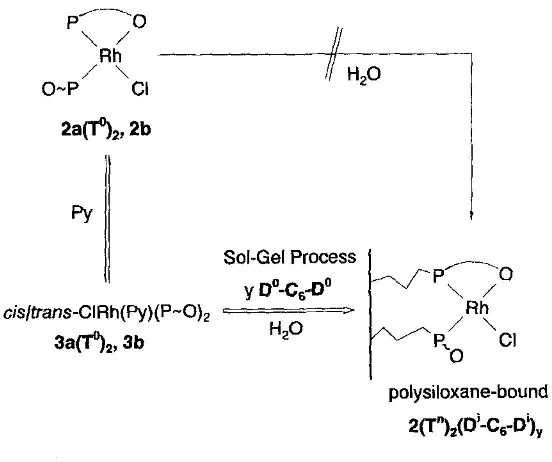

Composition of the Polycondensates

idealized $[\mathrm{Fn{-}SiO_{3/2}}][\mathrm{MeSiO_{2/2}(CH_2)_6O_{2/2}SiMe}]_y$

$\mathbf{2(T^3)_2(D^2{-}C_6{-}D^2)_y}$

realistic $[\mathrm{Fn{-}SiO_{n/2}(OX)_{3-n}}][\mathrm{MeSiO_{i/2}(OX)_{2-i}(CH_2)_6(XO)_{2-i}O_{i/2}SiMe}]_y$

$\mathbf{2(T^n)_2(D^i{-}C_6{-}D^i)_y}$

Scheme 4. Synthesis of the polysiloxane-bound chelated rhodium(I) complexes $\mathbf{2(T^n)_2(D^i{-}C_6{-}D^i)_y}$; *y* = number of co-condensed $\mathrm{D{-}C_6{-}D}$ molecules; *y* = 2, 8; *i*, *n* = number of Si-O-Si bonds; *i* = 0–2; *n* = 0–3; X = H, Me.

At 223 K the $^{31}\mathrm{P}\{^1\mathrm{H}\}$ NMR spectrum of $\mathbf{3a(T^0)_2}$ consists of a doublet [$\delta = 28.3$, $^1J(\mathrm{RhP}) = 167$ Hz] and the AB part of an ABX pattern [$\delta = 30.0$, $^1J(\mathrm{RhP}) = 193$ Hz; $\delta = 30.9$, $^1J(\mathrm{RhP}) = 162$ Hz, $^2J(\mathrm{PP}) = 49$ Hz]. The coupling constants of the ABX multiplet are in the same range as observed for the analogous complex *cis*-$[\mathrm{ClRh(Py)(PPh_3)_2}]$, and these signals can be assigned to the complex with a *cis* arrangement of the ether–phosphines.[33] The doublet corresponds to $\mathbf{3a(T^0)_2}$ with a *trans* configuration of the ligands.

Mixtures of $\mathbf{3a(T^0)_2}$ with variable amounts *y* of $\mathbf{D^0{-}C_6{-}D^0}$, water, the catalyst, and a minimum amount of MeOH underwent hydrolysis and polycondensation (Scheme 4). After approximately 14 hours a highly swollen gel was formed. Subsequent drying of the crude products and solvent processing (see Experimental Section) resulted in a complete elimination of the coordinated pyridine ligand and in the formation of the monochelated polysiloxane-bound complexes $\mathbf{2(T^n)_2(D^i{-}C_6{-}D^i)_y}$ (Table 1; Scheme 4, *y* = 2, 8). The orange polymers $\mathbf{2(T^n)_2(D^i{-}C_6{-}D^i)_y}$ are very air-sensitive powders. Two isotropic signals in the ^{31}P CP/MAS NMR spectrum of $\mathbf{2(T^n)_2(D^i{-}C_6{-}D^i)_2}$ (Figure 2A), with the same chemical shifts as those of its monomeric congener $\mathbf{2a(T^0)_2}$ (Table 2), are characteristic for one chelated and one nonchelated ligand. The additional peak at $\delta = 17$ in the ^{31}P CP/MAS NMR spectrum (Figure 2A) is assigned to the polysiloxane-bound binuclear species $[\{\mu\text{-ClRh}(P\sim O)_2\}_2]$. Owing to the enhanced chemical shift dispersion of the phosphorus nuclei in those amorphous materials, the coupling constants between rhodium and phosphorus are not resolved. This effect reduces the information deduced from solid state NMR spectra to the chemical shifts. When the sol–gel experiment was repeated with the nonhydrolyzable complex **3b**, **2b** was formed exclusively (Scheme 4). The chemical shifts in the $^{31}\mathrm{P}\{^1\mathrm{H}\}$ NMR spectrum of **2b** are compatible with those of $\mathrm{P^1}$ and $\mathrm{P^2}$ in the ^{31}P solid state NMR spectrum of $\mathbf{2(T^n)_2(D^i{-}C_6{-}D^i)_2}$ (Figure 2A).

Table 2. Comparison of the ^{31}P NMR data of the copolymers in the solid state with those of their monomeric counterparts in solution (coupling constants *J* in Hz).

Monomeric complex	$^{31}\mathrm{P}\{^1\mathrm{H}\}$ NMR δ	$^1J(\mathrm{RhP})$	$^2J(\mathrm{PP})$	Polymeric complex	^{31}P CP/MAS NMR, δ
$\mathbf{2a(T^0)_2}$ [a,b,c]	53.5	186.8	51.9	$\mathbf{2(T^n)_2(D^i{-}C_6{-}D^i)_2}$	57.9
	42.3	204.5	51.9		42.5
				$\mathbf{2(T^n)_2(D^i{-}C_6{-}D^i)_8}$	57.7
					43.0
$\mathbf{4a(T^0)_2}$ [d]	23.0	117.5		$\mathbf{4(T^n)_2(D^i{-}C_6{-}D^i)_2}$	22.1
$\mathbf{5a(T^0)_2}$ [a,b]	13.1	106.3		$\mathbf{5(T^n)_2(D^i{-}C_6{-}D^i)_2}$	11.7
$\mathbf{6a(T^0)_2}$ [d]	27.4	111		$\mathbf{6(T^n)_2(D^i{-}C_6{-}D^i)_2}$	25.9
$\mathbf{7a(T^0)_2}$ [d]	17.1	119.9		$\mathbf{7(T^n)_2(D^i{-}C_6{-}D^i)_2}$	15.7
$\mathbf{8a(T^0)_2}$ [a,e]	13.3	116.3		$\mathbf{8(T^n)_2(D^i{-}C_6{-}D^i)_2}$	12.9
$\mathbf{9a(T^0)_4}$ [a,b]	34.9	191			
	28.8	111.2		[f]	28.2

[a] The data set for only one of the of diastereomers are listed; for the other data sets, see Experimental Section. [b] In $[\mathrm{D_8}]$toluene. [c] At 243 K. [d] In $\mathrm{C_6D_6}$. [e] In $\mathrm{CD_2Cl_2}$. [f] The oxidative addition of $\mathrm{H_2}$ to $\mathbf{2(T^n)_2(D^i{-}C_6{-}D^i)_2}$ gives at least two compounds which cannot be characterized with satisfaction.

The dimerization of coordinatively unsaturated 14 electron rhodium(I) complex fragments of the type $[\mathrm{ClRh(PR_3)_2}]$ is a well-known phenomenon.[34–36] Some systems are binuclear in solution and in the solid state (e.g. $[\{\mu\text{-ClRh(PMe_3)_2}\}_2]$), and some mononuclear in both solution and the solid state (e.g. $[\mathrm{ClRh}(\overset{\frown}{PO})(P\sim O)]$, O,P = $i\mathrm{Pr_2PCH_2CH_2OCH_3}$).[24, 37] In be-

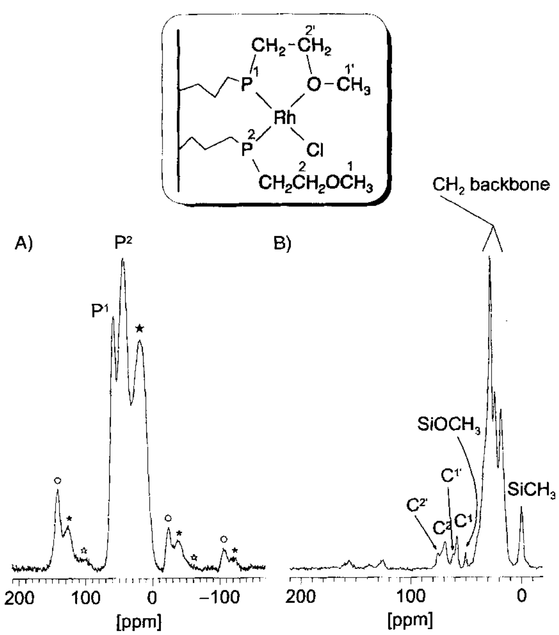

Figure 2. A) ^{31}P CP/MAS NMR spectrum of polysiloxane-bound $\mathbf{2(T^n)_2(D^i\text{-}C_6\text{-}D^i)_2}$ (ν_{rf} = 10 k Hz); B) the corresponding ^{13}C CP/MAS NMR spectrum. The filled star marks the signal for the dimeric species; the circle, asterisk, and outlined star denote spinning side bands.

tween these extremes, a series of complexes exist which are mononuclear or in equilibrium with their dimers in solution, and dimeric in the solid state (e.g. $[\{\mu\text{-ClRh(P}i\text{Pr}_3)_2\}_2]$, $[\{\mu\text{-ClRh(PCy}_3)_2\}_2]$). The degree of dimerization depends on the steric and electronic properties of the phosphine ligands. Since the monomeric complex $\mathbf{2a(T^0)_2}$ reacts with hydrogen with formation of the aforementioned binuclear complex $\mathbf{9a(T^0)_4}$ (Table 1; Scheme 3), steric reasons for the dimerization of $\mathbf{2(T^n)_2(D^i\text{-}C_6\text{-}D^i)_2}$ can be excluded. Also, it is rather unlikely that some other impurity is responsible for the signal at $\delta = 17$, because treatment of the polymer $\mathbf{2(T^n)_2(D^i\text{-}C_6\text{-}D^i)_2}$ with molecules like CO led to uniform reaction products (see below), and the simulation of the sol–gel conditions with **3b** (vide supra) did not show any indications of by-products. Moreover, the high-field shift of the resonance attributed to the polysiloxane-bound binuclear species $[\{\mu\text{-ClRh(P}\sim\text{O)}_2\}_2]$ relative to its mononuclear counterpart $\mathbf{2(T^n)_2(D^i\text{-}C_6\text{-}D^i)_2}$ is consistent with results reported elsewhere.[19]

A study of the ^{31}P CP/MAS NMR contact time variation performed for $\mathbf{2(T^n)_2(D^i\text{-}C_6\text{-}D^i)_2}$ revealed no significant differences in the cross-polarization dynamics of the various phosphorus species within the copolymer (see Experimental Section). Therefore the ratio of the mononuclear to the binuclear form was directly determined by peak deconvolution of the corresponding signals in the ^{31}P CP/MAS NMR spectrum of $\mathbf{2(T^n)_2(D^i\text{-}C_6\text{-}D^i)_2}$. Most of the complexes (67%)[38] are in the mononuclear form shown in Scheme 4.

A characteristic feature in the ^{13}C CP/MAS NMR spectrum of $\mathbf{2(T^n)_2(D^i\text{-}C_6\text{-}D^i)_2}$ is that the resonances of the ^{13}C signals of the OCH_2 and OCH_3 groups incorporated into the η^2-$\widehat{PO}$ ether–phosphine ligand are shifted downfield compared to the corresponding signals of the dangling ligand (P∼O) (Figure 2B, Table 3). No perceptible cleavage of Si–C and P–C bonds of the co-condensate and of the ligand takes place, since

Table 3. Comparison of selected ^{13}C NMR chemical shifts of the copolymers in the solid state with those of the corresponding monomers in solution.

Monomeric complex	$^{13}C\{^1H\}$ NMR CH_2O	 OCH_3	 RhC	Polymeric complex	^{13}C CP/MAS NMR CH_2O	 OCH_3	 RhC
$\mathbf{2a(T^0)_2}$ [a,b]	75.0	61.8		$\mathbf{2(T^n)_2(D^i\text{-}C_6\text{-}D^i)_2}$	75.1	61.2	
	71.7	58.5			68.8	57.9	
				$\mathbf{2(T^n)_2(D^i\text{-}C_6\text{-}D^i)_8}$	74.5	61.4	
					68.9	58.0	
$\mathbf{4a(T^0)_2}$ [c]	68.5	56.9	187.6 [d]	$\mathbf{4(T^n)_2(D^i\text{-}C_6\text{-}D^i)_2}$	68.6	58.1	188.0 [d]
$\mathbf{5a(T^0)_2}$ [a]	69.3	58.2	234.7 [e]	$\mathbf{5(T^n)_2(D^i\text{-}C_6\text{-}D^i)_2}$	68.2	58.3	230.7 [e]
$\mathbf{6a(T^0)_2}$ [c]	69.3	57.8	[f]	$\mathbf{6(T^n)_2(D^i\text{-}C_6\text{-}D^i)_2}$	68.6	58.0	[f]
$\mathbf{7a(T^0)_2}$ [c]	70.4	58.3	38.7 [g]	$\mathbf{7(T^n)_2(D^i\text{-}C_6\text{-}D^i)_2}$	68.5	58.0	[h]
$\mathbf{8a(T^0)_2}$ [i]	69.6	58.4	84.6 [j]	$\mathbf{8(T^n)_2(D^i\text{-}C_6\text{-}D^i)_2}$	67.9	58.0	85.6 [j]

[a] In $[D_8]$toluene. [b] At 243 K. [c] In C_6D_6. [d] RhCO (monomeric complex: dt, $^1J(RhC) = 74.0$, $^2J(PC) = 15.7$ Hz). [e] $Rh(CS_2)$ (monomeric complex: multiplet due to diastereomers). [f] The ^{13}C resonances of the coordinated pyridine are as follows: monomeric complex: $\delta = 154.0$ (*o*-C), 135.4 (*p*-C), 123.6 (*m*-C); polymeric complex: $\delta = 155.7$ (*o*-C), 136.5 (*p*-C), 124.4 (*m*-C). [g] $Rh(C_2H_4)$ (monomeric complex: d, $^1J(RhC) = 14.2$ Hz). [h] The resonances of the coordinated ethene carbon nuclei are hidden by those of the hydrocarbon backbone of the polysiloxane matrix. [i] In CD_2Cl_2. [j] Rh(-C≡C-) (monomeric complex: multiplet due to diastereomers).

the ^{13}C CP/MAS NMR spectrum shows the expected resonances of the $SiCH_2$ and $SiCH_3$ groups as well as those of the methylene groups of the hydrocarbon backbone (see Experimental Section). In the aromatic region of the ^{13}C CP/MAS NMR spectrum (Figure 2B) additional small peaks are observed, which are attributed to traces of pyridine remaining on the matrix. From the peaks of residual nonhydrolyzed methoxy substituents (Figure 2B) the degree of hydrolysis can be estimated:[39] $\mathbf{2(T^n)_2(D^i\text{-}C_6\text{-}D^i)_2}$, 97%; $\mathbf{2(T^n)_2(D^i\text{-}C_6\text{-}D^i)_8}$, 96%.

The real T:D ratios in the polysiloxane-bound complexes $\mathbf{2(T^n)_2(D^i\text{-}C_6\text{-}D^i)_y}$ were determined by ^{29}Si CP/MAS NMR spectroscopy (see Experimental Section). They are in acceptable agreement with the stoichiometries employed in the sol–gel process.

Reaction of the Polymer-Supported Complex $\mathbf{2(T^n)_2(D^i\text{-}C_6\text{-}D^i)_2}$ with Small Molecules: The polysiloxane-bound complex $\mathbf{2(T^n)_2(D^i\text{-}C_6\text{-}D^i)_2}$ was subjected to various catalytically interesting reactions, such as the coordination of CO, CS_2, ethene, tolan, and the oxidative addition of hydrogen in the presence and absence of additional pyridine (Scheme 5). The reaction with hydrogen can be regarded as a model reaction for the generation of the key intermediate $[ClRhH_2(olefin)(PR_3)_2]$, which is proposed to exist within the catalytic hydrogenation cycle.[40, 41] In particular, the accessibility of the rhodium centers to molecules of different size was investigated for various interphases. It is anticipated that the reactions in the interphase occur under mild conditions with cleavage of the Rh–O bond.

Reactions in Gaseous/Solid Interphases: When the dry solid $\mathbf{2(T^n)_2(D^i\text{-}C_6\text{-}D^i)_2}$ (stationary phase) was exposed to an atmosphere of carbon monoxide (mobile phase) at ambient temperature, the initial orange color rapidly turned to yellow, indicating the formation of the corresponding carbonyl rhodium(I) complex $\mathbf{4(T^n)_2(D^i\text{-}C_6\text{-}D^i)_2}$ (Table 1; Scheme 5). In the ^{31}P CP/MAS NMR spectrum of $\mathbf{4(T^n)_2(D^i\text{-}C_6\text{-}D^i)_2}$ (Figure 3A) one isotropic signal is observed at $\delta = 22.1$, which confirms a quantitative reaction. All the ^{13}C signals corresponding to the OCH_2 and OCH_3 groups appear at $\delta = 69.1$ and 58.1, respectively, and a

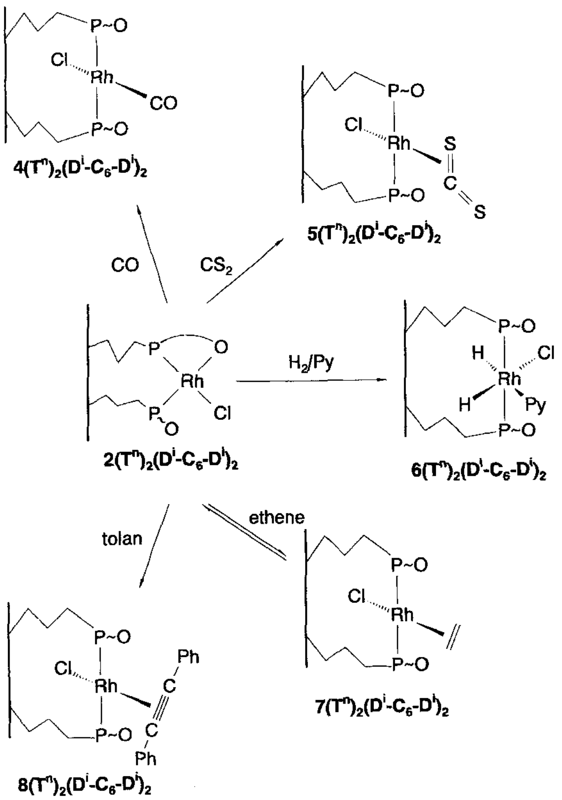

Scheme 5. Activation of small molecules in the interphase.

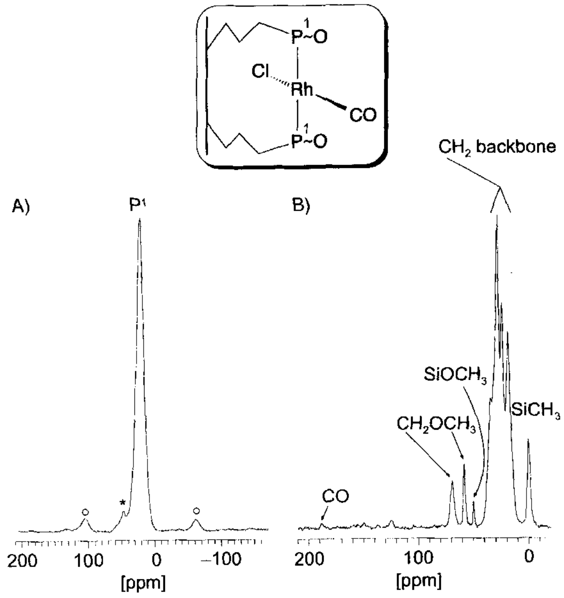

Figure 3. A) ^{31}P CP/MAS NMR spectrum of polysiloxane-bound 4(T^n)$_2$-(D^i-C$_6$-D^i)$_2$ (ν_{rf} = 10 k Hz) and B) the corresponding ^{13}C CP/MAS NMR spectrum; * = phosphine oxide; o = spinning side bands.

small new peak is observed at $\delta = 188.4$, which is assigned to the carbonyl C atom (Figure 3 B). All data sets of $\mathbf{4(T^n)_2(D^i\text{-}C_6\text{-}D^i)_2}$ are closely related to those of the corresponding monomer $\mathbf{4a(T^0)_2}$ (see Experimental Section), and the geometry depicted in Scheme 5 can thus be confirmed.

A cleavage of the Rh–O bond also took place on treatment of the copolymer $\mathbf{2(T^n)_2(D^i\text{-}C_6\text{-}D^i)_2}$ with ethene (1 bar) in the absence of solvent. The resulting polysiloxane-bound complex $\mathbf{7(T^n)_2(D^i\text{-}C_6\text{-}D^i)_2}$ (Table 1; Scheme 5) gives rise to one signal in the ^{31}P CP/MAS NMR spectrum with nearly the same chemical shift as its monomeric congener $\mathbf{7a(T^0)_2}$ in the corresponding ^{31}P{^{1}H} NMR spectrum (Table 2). Like $\mathbf{7a(T^0)_2}$, the yellow material $\mathbf{7(T^n)_2(D^i\text{-}C_6\text{-}D^i)_2}$ is only stable in the presence of ethene. Because the ethene pressure cannot be maintained during the transfer of the material into a zirconia rotor, the resonance peaks of the starting compound $\mathbf{2(T^n)_2(D^i\text{-}C_6\text{-}D^i)_2}$ (45%)[38] were also detected in the ^{31}P solid state NMR spectrum. However, the loss of ethene in the immobilized complex $\mathbf{7(T^n)_2(D^i\text{-}C_6\text{-}D^i)_2}$ occurred more slowly than in $\mathbf{7a(T^0)_2}$.

The copolymer $\mathbf{2(T^n)_2(D^i\text{-}C_6\text{-}D^i)_2}$ reacted smoothly with molecular hydrogen in an oxidative addition; a change of color from orange to yellow was observed. This was accompanied by the appearance of a broad absorption band at 2070 cm^{-1} in the hydride region of the IR spectrum. One broad peak in the corresponding ^{31}P CP/MAS NMR spectrum at $\delta = 28$ (Table 2) points to the generation of at least two compounds within the material. From the present data no definitive conclusions can be drawn about the types and geometries of these complexes.

Reactions in Liquid/Solid Interphases: When the oxidative addition of hydrogen was performed with a suspension of $\mathbf{2(T^n)_2(D^i\text{-}C_6\text{-}D^i)_2}$ (stationary phase) in ethanol/pyridine (mobile phase), $\mathbf{6(T^n)_2(D^i\text{-}C_6\text{-}D^i)_2}$ was obtained, which contains octahedrally configurated centers (Scheme 5). The yellow powder is characterized by the appearance of one signal in the ^{31}P CP/MAS NMR spectrum (Table 2) and by the expected resonances of the coordinated pyridine ligand in the ^{13}C CP/MAS NMR spectrum (Table 3). The RhH$_2$ band (2056 cm^{-1}) in the IR spectrum provides further evidence for the existence of $\mathbf{6(T^n)_2(D^i\text{-}C_6\text{-}D^i)_2}$. All measured data are compatible with those of the monomeric congener and establish the geometry displayed in Scheme 5.

Upon treatment of a suspension of $\mathbf{2(T^n)_2(D^i\text{-}C_6\text{-}D^i)_2}$ in *n*-hexane at 243 K with CS$_2$ (mobile phase) the polysiloxane-bound η^2-(CS) carbon disulfide complex $\mathbf{5(T^n)_2(D^i\text{-}C_6\text{-}D^i)_2}$, which is orange-brown and temperature-labile, was generated in the interphase. Its ^{31}P CP/MAS NMR spectrum shows one peak at the same position as the doublet of the monomeric complex $\mathbf{5a(T^0)_2}$ in the ^{31}P{^{1}H} NMR spectrum; this confirms the geometry of the CS$_2$ adduct $\mathbf{5(T^n)_2(D^i\text{-}C_6\text{-}D^i)_2}$ (Table 2; Scheme 5). The ^{13}C CP/MAS NMR (Table 3) and IR data (Experimental Section) of $\mathbf{5(T^n)_2(D^i\text{-}C_6\text{-}D^i)_2}$ provide additional evidence for its formation.

At ambient temperature the reaction of the swollen gel $\mathbf{2(T^n)_2(D^i\text{-}C_6\text{-}D^i)_2}$ in toluene with diphenylacetylene in the same solvent (mobile phase) afforded the yellow η^2-diphenylacetylene complex $\mathbf{8(T^n)_2(D^i\text{-}C_6\text{-}D^i)_2}$ (Scheme 5). In Figure 4A the ^{31}P solid state NMR spectrum displays mainly one peak attributed to this supported compound (Table 2). Besides the signal of the converted complex $\mathbf{8(T^n)_2(D^i\text{-}C_6\text{-}D^i)_2}$, those of the starting material $\mathbf{2(T^n)_2(D^i\text{-}C_6\text{-}D^i)_2}$ are still present. After deconvolution of the ^{31}P CP/MAS NMR spectrum the amount of the tolan complex within the material was estimated at 75%.[38] Clearly most of the rhodium atoms within the matrix are accessible even for the bulky tolan molecules. The resonances of the coordinated quaternary alkyne carbon atoms and the resonance of the

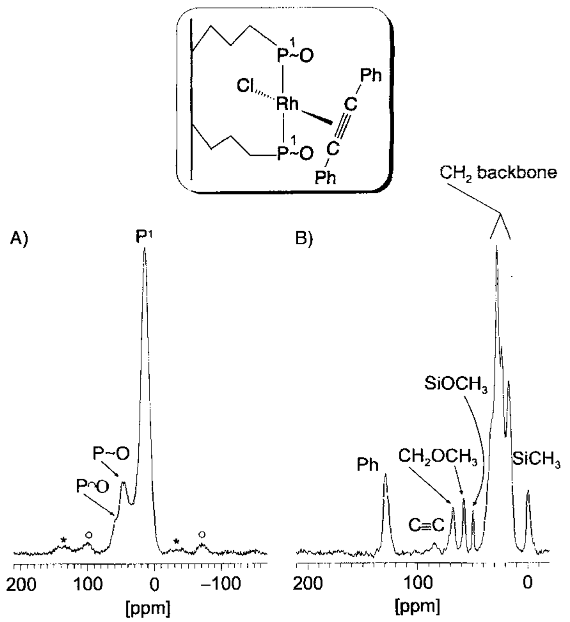

Figure 4. A) ^{31}P CP/MAS NMR spectrum of polysiloxane-bound $\mathbf{8(T^{n})_{2}(D^{i}\text{-}C_{6}\text{-}D^{i})_{2}}$ ($\nu_{rf} = 10$ k Hz) and B) the corresponding ^{13}C CP/MAS NMR spectrum; ○ and * denote spinning side bands.

phenyl groups of the tolan molecule in the ^{13}C CP/MAS NMR spectrum (Figure 4B; Table 3) are consistent with the structure of $\mathbf{8(T^{n})_{2}(D^{i}\text{-}C_{6}\text{-}D^{i})_{2}}$. Recently it was demonstrated that increasing the temperature or amount of the co-condensation agent D-C$_6$-D results in higher mobilities of the Fn–T/D-C$_6$-D copolymers.[10] It is assumed that more mobile materials lead to a better accessibility of the reaction centers in the stationary phase. Therefore, the observed value for $\mathbf{8(T^{n})_{2}(D^{i}\text{-}C_{6}\text{-}D^{i})_{2}}$ is considered to be at the lower limit for accessibility. This suggestion is corroborated by the results of the catalytic hydrogenation experiments (vide infra).

Catalytic Hydrogenation of Tolan in the Interphase: The polysiloxane-bound rhodium(I) complexes $\mathbf{2(T^{n})_{2}(D^{i}\text{-}C_{6}\text{-}D^{i})_{2}}$ and $\mathbf{2(T^{n})_{2}(D^{i}\text{-}C_{6}\text{-}D^{i})_{8}}$ (stationary phases) proved to be efficient catalysts in the hydrogenation of diphenylacetylene in organic solvents (mobile phases) under very mild conditions, typically at 303 K and 5 bar H$_2$. The selectivity toward *cis*-stilbene was high (usually 98%), as long as the conversion of tolan did not exceed 95%.

Several observations support the assumption that the catalytically active species is an immobilized rhodium complex and that the tolan complex $\mathbf{8(T^{n})_{2}(D^{i}\text{-}C_{6}\text{-}D^{i})_{2}}$ (Scheme 5) is involved in the catalytic cycle:

1) The hydrogenation of the alkyne, perceptible by the pressure drop inside the autoclave, started instantaneously after addition of hydrogen, that is, there is no activation period.
2) After hydrogenations with incomplete conversions, the tolan complex $\mathbf{8(T^{n})_{2}(D^{i}\text{-}C_{6}\text{-}D^{i})_{2}}$ could be recovered; this was demonstrated by IR and ^{31}P CP/MAS NMR spectroscopy.
3) Even small amounts of carbon monoxide mixed in with the hydrogen completely deactivated the catalyst, owing to the quantitative and irreversible formation of the carbonyl complex $\mathbf{4(T^{n})_{2}(D^{i}\text{-}C_{6}\text{-}D^{i})_{2}}$ (Scheme 5).
4) When the polymer was recovered from the reaction mixture and then used again in a reaction with new solvent and tolan, hydrogenation was observed with identical selectivities and only slightly smaller conversions (Table 4). This insignificant drop of activity is traced back to a partial oxidation of the air-sensitive metal complex during catalyst separation.

Table 4. Conversions and selectivities of four consecutive hydrogenation runs with a recycling of the catalyst $\mathbf{2(T^{n})_{2}(D^{i}\text{-}C_{6}\text{-}D^{i})_{2}}$ [a].

Run no.	Conversion [%]	*cis*-Stilbene [%]	*trans*-Stilbene [%]	Bibenzyl [%]	TON [b]	TOF [c]
1	92.1	97.8	1.8	0.4	143	190
2	95.0	97.5	2.0	0.6	147	196
3	88.5	98.2	1.5	0.3	137	183
4	82.5	98.2	1.5	0.3	128	171

[a] Reaction conditions: 303 K, 5 bar H$_2$, 45 min, 30 mL methanol:toluene = 1:1, tolan:rhodium = 155:1. [b] Turnover number [$\text{mol}_{\text{sub}}\,\text{mol}_{\text{cat}}^{-1}$]. [c] Turnover frequency [$\text{mol}_{\text{sub}}\,\text{mol}_{\text{cat}}^{-1}\,\text{h}^{-1}$].

5) The reaction solutions of four consecutive hydrogenation runs were separated from the polymer, concentrated, and subjected again to the reaction conditions described above, in the absence of the polymer. No further hydrogenation of remaining tolan took place. Therefore, the catalytically active species cannot be a soluble metal complex which might be formed under the reducing conditions by the negligible leaching of rhodium from the matrix (only 2.5% rhodium was found to be detached from the support).

In order to investigate the differences in the catalytic behavior of $\mathbf{2(T^{n})_{2}(D^{i}\text{-}C_{6}\text{-}D^{i})_{y}}$ ($y = 2, 8$) with varying conditions, such as pressure, temperature, solvent, and content (y) of the co-condensate, the reaction was stopped after 20 minutes. The comparison of the observed conversions and selectivities are described below.

Influence of hydrogen pressure: An increase of the hydrogen pressure led to an increase in conversion. However, this effect is less pronounced than expected. On doubling the pressure from 20 to 40 bar, the hydrogenation was not accelerated significantly. This result shows that the oxidative addition of hydrogen is not the rate-determining step of the reaction. As expected, the increase in pressure was accompanied by a slight drop in the selectivity from 99 to 97.6% for *cis*-stilbene (Figure 5, Table 5).

Influence of temperature: A linear relationship between the conversion and the reaction temperature was established. Again, the gradient of the plot of conversion versus temperature is smaller than expected, and the increase in temperature is accompanied by a slight decline in selectivity (Figure 6, Table 6). Our explanation for the relatively small influence of temperature and pressure on the turnover rate is that the diffusion of the rather bulky tolan molecules through the polysiloxane matrix is the rate-determining step, rather than any elementary step within the catalytic cycle.

Influence of solvent: A significant increase in conversion was observed with increasing amounts of methanol in the toluene/

methanol solvent mixture (Figure 7, Table 7). A similar increase in reaction rate was observed with increasing solvent polarity (toluene, THF, ethanol, methanol; Figure 8, Table 8). This is another example for the common phenomenon, namely, that many transition metal catalyzed hydrogenations are favored in polar solvents, especially in alcohols.

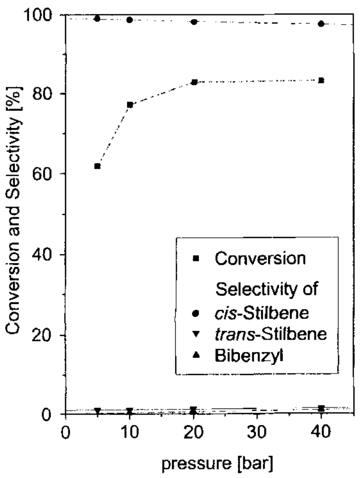

Figure 5. Dependence of conversion and selectivity on pressure in the hydrogenation of tolan catalyzed by $\mathbf{2(T^n)_2(D^i\text{-}C_6\text{-}D^i)_2}$ (for reaction conditions, see Table 5).

Table 5. Influence of the hydrogen pressure on conversion and selectivity [a].

P [bar]	Conversion [%]	*cis*-Stilbene [%]	*trans*-Stilbene [%]	Bibenzyl [%]	TON [b]	TOF [c]
5	61.9	99.0	1.0	–	96	288
10	77.2	98.7	1.0	0.3	120	359
20	83.0	98.1	1.3	0.6	129	386
40	88.3	97.6	1.4	1.0	137	411

[a] Reaction conditions: 303 K, 20 min, 30 mL methanol:toluene = 1:1, tolan:rhodium catalyst $\mathbf{2(T^n)_2(D^i\text{-}C_6\text{-}D^i)_2}$ = 155:1. [b] Turnover number [$\mathrm{mol_{sub}\,mol_{cat}^{-1}}$]. [c] Turnover frequency [$\mathrm{mol_{sub}\,mol_{cat}^{-1}\,h^{-1}}$].

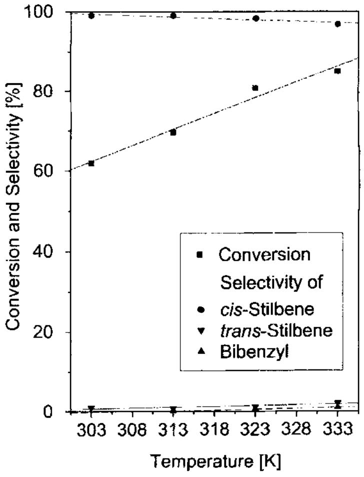

Figure 6. Dependence of conversion and selectivity on temperature in the hydrogenation of tolan catalyzed by $\mathbf{2(T^n)_2(D^i\text{-}C_6\text{-}D^i)_2}$ (for reaction conditions, see Table 6).

Table 6. Influence of the temperature on conversion and selectivity [a].

T [K]	Conversion [%]	*cis*-Stilbene [%]	*trans*-Stilbene [%]	Bibenzyl [%]	TON [b]	TOF [c]
303	61.9	99.0	1.0	–	96	288
313	69.9	99.0	0.8	0.2	108	325
323	80.8	98.3	1.2	0.5	125	376
333	85.0	96.8	2.2	1.0	132	395

[a] Reaction conditions: 5 bar H_2, 20 min, 30 mL methanol/toluene 1:1, tolan:rhodium catalyst $\mathbf{2(T^n)_2(D^i\text{-}C_6\text{-}D^i)_2}$ 155:1. [b] Turnover number [$\mathrm{mol_{sub}\,mol_{cat}^{-1}}$]. [c] Turnover frequency [$\mathrm{mol_{sub}\,mol_{cat}^{-1}\,h^{-1}}$].

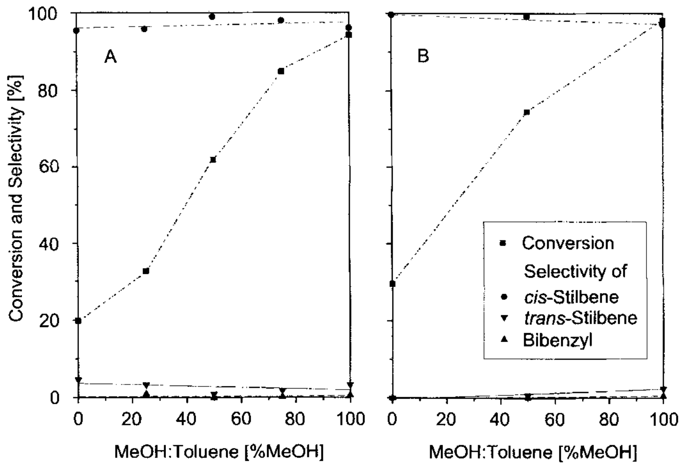

Figure 7. Dependence of conversion and selectivity on the composition of the solvent in the hydrogenation of tolan catalyzed by $\mathbf{2(T^n)_2(D^i\text{-}C_6\text{-}D^i)_y}$ [y = 2 (A), 8 (B)] (for reaction conditions, see Table 7).

Table 7. Influence of the amount of the co-condensation agent and of the solvent composition on conversion and selectivity [a].

Catalyst	MeOH [%] [b]	Conversion [%]	*cis*-Stilbene [%]	*trans*-Stilbene [%]	Bibenzyl [%]	TON [c]	TOF [d]
$\mathbf{2(T^n)_2(D^i\text{-}C_6\text{-}D^i)_2}$	0	19.9	95.4	4.6	–	31	93
	25	32.7	95.8	3.3	0.9	51	152
	50	61.9	99.0	1.0	–	96	288
	75	85.0	98.0	1.8	0.2	132	395
	100	94.3	96.1	3.3	0.6	146	438
$\mathbf{2(T^n)_2(D^i\text{-}C_6\text{-}D^i)_8}$	0	29.5	99.6	0.4	–	46	137
	50	74.7	99.2	0.7	0.1	116	347
	100	98.2	97.1	2.4	0.5	152	457

[a] Reaction conditions: 303 K, 5 bar H_2, 20 min, tolan:rhodium = 155:1. [b] Content of methanol in a 30 mL mixture of methanol and toluene. [c] Turnover number [$\mathrm{mol_{sub}\,mol_{cat}^{-1}}$]. [d] Turnover frequency [$\mathrm{mol_{sub}\,mol_{cat}^{-1}\,h^{-1}}$].

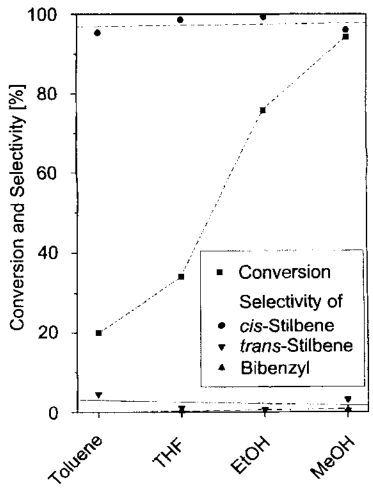

Figure 8. Dependence of conversion and selectivity on the polarity of the solvent in the hydrogenation of tolan catalyzed by $\mathbf{2(T^n)_2(D^i\text{-}C_6\text{-}D^i)_2}$ (for reaction conditions, see Table 8).

Table 8. Influence of the solvent on conversion and selectivity [a].

Solvent	Conversion [%]	*cis*-Stilbene [%]	*trans*-Stilbene [%]	Bibenzyl [%]	TON [b]	TOF [c]
toluene	19.9	95.4	4.6		31	93
THF	34.2	98.6	1.1	0.3	53	159
ethanol	75.8	99.3	0.7	–	117	352
methanol	94.3	96.1	3.3	0.6	146	438

[a] Reaction conditions: 303 K, 5 bar H_2, 20 min, 30 mL solvent, tolan:rhodium catalyst $\mathbf{2(T^{n})_2(D^{i}\text{-}C_6\text{-}D^{i})_2}$ 155:1. [b] Turnover number [$\mathrm{mol_{sub}\,mol_{cat}^{-1}}$]. [c] Turnover frequency [$\mathrm{mol_{sub}\,mol_{cat}^{-1}\,h^{-1}}$].

Influence of co-condensate: Raising the ratio of co-condensate $\mathbf{D^0\text{-}C_6\text{-}D^0}$ to $\mathbf{2\,a(T^0)_2}$ from 2:1 to 8:1 generally led to an increase of turnover frequency (Table 7). This result can be traced back to the better accessibility of the rhodium centers within the stationary phase in the more flexible polysiloxane framework.[10] It is noteworthy that the enhancement of the reaction rate was more conspicuous for toluene than for methanol. This observation can be explained by the fact that the relatively nonpolar carrier swells to a greater extent in the less polar solvent, and this partially compensates the faster catalytic hydrogenation in the more polar solvent.

Table 9. Influence of the ratio (*r*) of tolan to catalyst $\mathbf{2(T^{n})_2(D^{i}\text{-}C_6\text{-}D^{i})_2}$ on conversion and selectivity [a].

r	*t* [min]	Conversion [%]	*cis*-Stilbene [%]	*trans*-Stilbene [%]	Bibenzyl [%]	TON [b]	TOF [c]
155:1	20	61.9	99.0	1.0	–	96	288
1000:1	120	89.9	98.3	1.3	0.4	899	449

[a] Reaction conditions: 303 K, 5 bar H_2, 30 mL methanol:toluene = 1:1. [b] Turnover number [$\mathrm{mol_{sub}\,mol_{cat}^{-1}}$]. [c] Turnover frequency [$\mathrm{mol_{sub}\,mol_{cat}^{-1}\,h^{-1}}$].

Influence of tolan: catalyst ratio: A higher tolan:catalyst ratio of 1000:1 instead of 155:1 noticeably increased the turnover frequency to more than 400 $\mathrm{mol_{sub}\,mol_{cat}{}^{-1}\,h^{-1}}$ (Table 9). This can be explained by the higher gradient of tolan concentration between the solution and the active center, which results in a faster diffusion of substrate molecules to the catalyst within the matrix.

Influence of the immobilization: The comparison of the catalytic activity of the monomeric precursor complex $\mathbf{2\,a(T^0)_2}$ with that of its immobilized counterpart $\mathbf{2(T^{n})_2(D^{i}\text{-}C_6\text{-}D^{i})_2}$ under identical conditions gave a surprising result: the turnover frequency of the monomeric catalyst was only about half that of the polymer. This difference cannot be explained by cocatalytic effects of traces of water or tin compounds, which might still be adsorbed on the carrier after polycondensation, because the controlled addition of water and $(n\mathrm{Bu})_2\mathrm{Sn(OAc)}_2$ to the reaction mixture of the homogeneous catalyst $\mathbf{2\,a(T^0)_2}$ did not change the reaction rate at all. Also, the lower activity cannot be attributed to coordination of the silicon-bound methoxy groups to the rhodium center in $\mathbf{2\,a(T^0)_2}$; an experiment with the analogous trimethylsilyl-functionalized complex **2b** under the same conditions afforded the same conversion. The enhancement of catalytic activity upon immobilization of a transition metal complex has been observed in other cases.[42, 43] As described above the monomeric monochelated complex $\mathbf{2\,a(T^0)_2}$ dimerizes quantitatively under an atmosphere of hydrogen to form the mixed-valence binuclear dihydrido species $\mathbf{9\,a(T^0)_4}$ (Scheme 3). Such binuclear complexes are less active in catalysis.[44] We assume that the immobilization of the monochelated rhodium complex $\mathbf{2\,a(T^0)_2}$ prevents the dimerization of the spatially separated mononuclear metal complexes within the polymer $\mathbf{2(T^{n})_2(D^{i}\text{-}C_6\text{-}D^{i})_2}$. Hence $\mathbf{2(T^{n})_2(D^{i}\text{-}C_6\text{-}D^{i})_2}$ provides a larger number of catalytically active mononuclear rhodium centers. Another reason that might contribute to the change in catalytic activity after immobilization is a higher reaction temperature around the polymerized complex centers, due to the reaction enthalpy produced within the rather small volume of the polymer particles.

Conclusion

The sol–gel process has been shown to be an excellent method for the design of tailored stationary phases containing reactive transition metal complexes. The sol–gel conditions can be adapted to the particular requirements of the monomeric precursor complex $[\mathrm{ClRh}(\overset{\frown}{\mathrm{PO}})(\mathrm{P}\sim\mathrm{O})]$ [$\mathbf{2\,a(T^0)_2}$], so that even this sensitive, coordinatively unsaturated, pseudo 14 electron rhodium(I) complex can be incorporated into a polysiloxane matrix. The matrix was modified by employing the co-condensation agent $\mathbf{D^0\text{-}C_6\text{-}D^0}$ during the polycondensation reaction. In this way, organic–inorganic hybrid polymer networks were obtained, which are highly cross-linked, but still have sufficient mobility and swelling capacity. This is the main reason why the rhodium atoms within these novel stationary phases are readily accessible for small molecules like CO, ethene, CS_2, and H_2/pyridine. This was demonstrated by their stoichiometric reactions in solid/gaseous and solid/liquid interphases. It was concluded that the accessibility of the reactive centers for the rather bulky tolan molecules is at least 75%. Various catalytically important reaction steps, such as the coordination of olefins and alkynes to the reaction center, were found to take place in the interphase in a similar manner to the reactions in solution. The organometallic–organic hybrid polymers $\mathbf{2(T^{n})_2(D^{i}\text{-}C_6\text{-}D^{i})_{\mathit{y}}}$ displayed high turnover frequencies and selectivities in the hydrogenation of tolan under very mild conditions. The reaction rates were found to depend on the various factors that affect the rate of diffusion of the substrate into the polysiloxane, above all the content of co-condensation agent in the polymer and the solvent polarity; the conditions influencing the reaction rates within the catalytic cycle (hydrogen pressure and temperature) have a less pronounced effect. Therefore, the diffusion of the tolan to the rhodium centers within the polymers $\mathbf{2(T^{n})_2(D^{i}\text{-}C_6\text{-}D^{i})_{\mathit{y}}}$ is considered to be the rate-determining step. The immobilization of the rhodium complex markedly enhances the catalytic activity with respect to that of the monomeric precursor $\mathbf{2\,a(T^0)_2}$. This phenomenon can be explained by the fact that immobilization prevents the catalytically inactive binuclear hydrido species from being generated.

Experimental Section

Characterization: The elemental analyses were carried out on a Carlo Erba analyzer, Model 1106. The surface areas were determined by analyzing the N_2 adsorption isotherms according to the BET method using a Micromeritics

Gemini II. For the photochemical reactions a Heraeus Hg high-pressure lamp of the type TQ150 Original Hanau was employed. IR data were obtained on a Bruker IFS 48 FT-IR spectrometer. The solution nuclear magnetic resonance spectra (NMR) were recorded on a Bruker AC80 [$^{31}P\{^1H\}$; at 243 K] and a Bruker DRX 250 spectrometer [$^{31}P\{^1H\}$, $^{13}C\{^1H\}$, ^1H; at 296 K, unless otherwise noted). The frequencies and standards are as follows: $^{31}P\{^1H\}$ NMR: 32.44 and 101.25 MHz, external 85% H_3PO_4 in [D_6]acetone. $^{13}C\{^1H\}$ NMR: 62.90 MHz. ^1H NMR: 250.13 MHz. The chemical shifts in the $^{13}C\{^1H\}$ and ^1H NMR spectra were measured relative to partially deuterated solvent peaks, which are reported relative to TMS. The 2 D $^{31}P,^{31}P\{^1H\}$ COSY NMR spectrum of compound **2a(T⁰)₂** was recorded on the Bruker DRX250 spectrometer. Mass spectra (field desorption) were acquired on a Finnigan MAT711A modified by the AMD measurement and data systems (8 kV, 30 °C) and reported as mass/charge (*m/z*).
The CP/MAS solid state NMR spectra were recorded on a Bruker MSL200 [^{29}Si] and a Bruker ASX300 [^{13}C and ^{31}P] multinuclear spectrometer equipped with wide-bore magnets (field strengths: 4.7 and 7.05 T). Magic angle spinning was applied at 3 (^{29}Si) and 10 kHz (^{31}P, ^{13}C). All measurements were carried out under exclusion of molecular oxygen. Frequencies and standards: ^{29}Si, 39.75 MHz (Q_8M_8); ^{13}C, 75.47 MHz [TMS, carbonyl resonance of glycine ($\delta = 176.03$) as the second standard]; ^{31}P, 121.49 MHz [85% H_3PO_4, $NH_4H_2PO_4$ ($\delta = 0.8$) as the second standard]. The cross-polarization constant T_{PH} of $\mathbf{2(T^n)_2(D^i\text{-}C_6\text{-}D^i)_2}$ was determined by variation of the contact time T_c (22 experiments). The proton relaxation time in the rotating frame was measured by direct proton spin lock–τ–CP experiments as described by Schaefer and Stejskal.[45] The relaxation time data were obtained by using the Bruker software SIMFIT or Jandel software PEAKFIT. For quantification of the silyl species in $\mathbf{2(T^n)_2(D^i\text{-}C_6\text{-}D^i)_2}$ and $\mathbf{2(T^n)_2(D^i\text{-}C_6\text{-}D^i)_8}$, ^{29}Si CP/MAS NMR spectra at a contact time T_c of 4 ms were recorded by accumulating 7000–12000 fid's until acceptable signal/noise ratios were obtained. Peak deconvolution of the spectra was performed with the Bruker software XNMR using Voigtian line shapes. The relative amounts I_0 of each of the D^0, D^1, D^2, T^1, T^2, and T^3 species in one sample were calculated by known methods.[38c, 46, 47]

Catalysis: The hydrogenation experiments were carried out in a 100 mL steel autoclave equipped with a magnetic stirring bar. The autoclave was evacuated and flushed with argon three times before the reaction mixture was introduced [31–56 µmol catalyst with respect to rhodium, 4.75–8.68 mmol of tolan (ratio Rh:substrate 1:155) in the solvent (30 mL) unless otherwise noted]. After being heated to the desired temperature, the suspension was set under hydrogen pressure and stirred. The analyses were performed quantitatively on a GC6000 Vega Series 2 (Carlo Erba Instruments) with an FID and a capillary column CP Sil 88 [17 m; carrier gas, He (50 kPa); integrator, Hewlett Packard 3390A]. The amount of detached rhodium was determined with a Perkin-Elmer Modell 4000 atomic absorption spectrometer.

General Methods: All manipulations were performed under argon by employing the usual Schlenk techniques. Methanol was dried with magnesium and distilled, and ethanol was distilled from NaOEt. *n*-Hexane and toluene were distilled from sodium benzophenone ketyl. H_2O and $(nBu)_2Sn(OAc)_2$ were distilled under inert gas prior to use. All solvents were stored under argon. The monomeric co-condensation agent $\mathbf{D^0\text{-}C_6\text{-}D^0}$ and the starting complex $[\{\mu\text{-}ClRh(COE)_2\}_2]$ were synthesized as described previously.[10, 48]

Synthesis of Ligands 1a(T⁰) and 1b: A solution of *n*BuLi in *n*-hexane (113 mL of a 1.6 M solution) was added dropwise to a solution of $C_6H_{11}PH_2$ (20.0 g, 172 mmol) in THF (200 mL) at 0 °C. The yellow solution containing $C_6H_{11}PH(Li)$ was allowed to warm up to room temperature and stirred for 30 min. It was then refluxed for 1 h and cooled down to room temperature. $ClCH_2CH_2OCH_3$ (16.1 g, 172 mmol) was added dropwise within 1 h. The solution was stirred for another 30 min under reflux to complete the reaction and then cooled down to room temperature. To the colorless reaction mixture a degassed aqueous solution saturated with NH_4Cl (250 mL) was added, and the organic layer was separated. The organic solution was dried ($NaSO_4$) and separated from the solid residue. After evaporation of the volatiles under vacuum the crude product was distilled under vacuum to yield 22.5 g (75%) of the intermediate $C_6H_{11}PH(CH_2CH_2OCH_3)$ as a colorless air-sensitive oil. B.p. 329 K; $^{31}P\{^1H\}$ NMR (32.44 MHz, acetone): $\delta = -61.8$. In a quartz Schlenk tube the specified amount of $C_6H_{11}PH(CH_2CH_2OCH_3)$ and the corresponding allylsilane $CH_2{=}CHCH_2SiR_3$ [R = OMe (**a**), Me (**b**)] were stirred and subjected to UV irradiation ($\lambda = 254$ nm) for 18 h. The distillation of the product mixtures under vacuum afforded analytically pure colorless liquids.

Cyclohexyl(2-methoxyethyl)(3-(trimethoxysilyl)propyl)phosphine [1a(T⁰)]: The photochemical treatment of $C_6H_{11}PH(CH_2CH_2OCH_3)$ (13.6 g, 78 mmol) and allyltrimethoxysilane (13.5 g, 83 mmol) and subsequent distillation under vacuum gave 19 g (72%) of **1a(T⁰)** as an air-sensitive oil. B.p. 398–408 K; $^{31}P\{^1H\}$ NMR (101.25 MHz, C_6D_6): $\delta = -22.9$; $^{13}C\{^1H\}$ NMR (C_6D_6): $\delta = 71.7$ (d, $^2J(P,C) = 23.9$ Hz; $PCH_2\mathit{C}H_2OCH_3$), 58.3 (s; $PCH_2CH_2O\mathit{C}H_3$), 50.4 (s; $SiOCH_3$), 35.8 (d, $^1J(P,C) = 12.0$ Hz; PCH of C_6H_{11}), 25.5–29.9 (m; $P\mathit{C}H_2CH_2OCH_3$, $P\mathit{C}H_2CH_2CH_2Si$, 5 CH_2 of C_6H_{11}), 20.5 (d, $^2J(P,C) = 17.0$ Hz; $PCH_2\mathit{C}H_2CH_2Si$), 11.9 (d, $^3J(P,C) = 10.7$ Hz; $PCH_2CH_2\mathit{C}H_2Si$); ^1H NMR (C_6D_6): $\delta = 3.40$–3.53 (m, 2H; $PCH_2C\mathit{H}_2OCH_3$), 3.44 (s, 9H; $SiOCH_3$), 3.14 (s, 3H; $PCH_2CH_2OC\mathit{H}_3$), 1.10–1.80 (m, 17H; $PC\mathit{H}_2CH_2OCH_3$, $PC\mathit{H}_2C\mathit{H}_2CH_2Si$, C_6H_{11}), 0.81–0.87 (m, 2H; $PCH_2CH_2C\mathit{H}_2Si$); MS (FD): *m/z* (%): 336 (100) [M^+]; $C_{15}H_{33}O_4PSi$ (336.5): calcd C 53.54, H 9.89; found C 53.85, H 10.24.

Cyclohexyl(2-methoxyethyl)(3-(trimethylsilyl)propyl)phosphine [1b]: The photochemical treatment of $C_6H_{11}PH(CH_2CH_2OCH_3)$ (9.4 g, 54 mmol) and allyltrimethylsilane (6.6 g, 58 mmol) and subsequent distillation under vacuum gave 9.1 g (58%) of **1b** as an air-sensitive oil. B.p. 403–413 K; $^{31}P\{^1H\}$ NMR (101.25 MHz, C_6D_6): $\delta = -22.9$; $^{13}C\{^1H\}$ NMR (C_6D_6): $\delta = 71.8$ (d, $^2J(P,C) = 24.5$ Hz; $PCH_2\mathit{C}H_2OCH_3$), 58.4 (s; $PCH_2CH_2O\mathit{C}H_3$), 36.0 (d, $^1J(P,C) = 12.0$ Hz; PCH of C_6H_{11}), 25.7–29.9 (m; $P\mathit{C}H_2CH_2OCH_3$, $P\mathit{C}H_2CH_2CH_2Si$, 5 CH_2 of C_6H_{11}), 21.7 (d, $^2J(P,C) = 16.4$ Hz; $PCH_2\mathit{C}H_2CH_2Si$), 19.3 (d, $^3J(P,C) = 9.4$ Hz; $PCH_2CH_2\mathit{C}H_2Si$), −1.3 (s; $SiCH_3$); ^1H NMR (C_6D_6): $\delta = 3.46$–3.55 (m, 2H; $PCH_2C\mathit{H}_2OCH_3$), 3.15 (s, 3H; $PCH_2CH_2OC\mathit{H}_3$), 1.15–1.80 (m; 17H; $PC\mathit{H}_2CH_2OCH_3$, $PC\mathit{H}_2C\mathit{H}_2CH_2Si$, C_6H_{11}), 0.60–0.66 (m; 2H; $PCH_2CH_2C\mathit{H}_2Si$), 0.0 (s, 9H; $SiCH_3$); MS (FD): *m/z* (%): 288 (100) [M^+]; $C_{15}H_{33}OPSi$ (288.5): calcd C 62.45, H 11.53; found C 62.22, H 11.60.

Synthesis of the Monomeric Complexes 2a(T⁰)₂ and 2b: The specified amounts of the ligand **1a(T⁰)** or **1b** were added to a suspension of the corresponding amount of $[\{\mu\text{-}ClRh(COE)_2\}_2]$ in acetone (6 mL). The reaction mixtures were stirred for 20 min at 273 K. After evaporation of the solvent under vacuum orange viscous oils were obtained. The very air-sensitive oils were dissolved in *n*-hexane (6 mL), and the mixtures again treated under vacuum to remove all volatiles. This procedure was repeated, and the products were subsequently dried under vacuum for 4 h.

Chlorobis[cyclohexyl(2-methoxyethyl)(3-(trimethoxysilyl)propyl)phosphine-*P;O′,P′*]rhodium(I) [2a(T⁰)₂]: The reaction of **1a(T⁰)** (134 mg, 0.4 mmol) with $[\{\mu\text{-}ClRh(COE)_2\}_2]$ (72 mg, 0.1 mmol) gave 162 mg of **2a(T⁰)₂** (100%). $^{31}P\{^1H\}$ NMR (101.25 MHz, [D_8]toluene): δ (diastereomer II) = 53.7 (dd, $^1J(Rh,P) = 185.5$ Hz, $^2J(P,P) = 52.1$), 38.3 (dd, $^1J(Rh,P) = 203.2$ Hz, $^2J(P,P) = 52.1$); $^{13}C\{^1H\}$ NMR ([D_8]toluene): $\delta = 50.5$ (s; $SiOCH_3$), 35.8 (m; PCH of C_6H_{11}), 25.5–29.9 (m; $P\mathit{C}H_2CH_2OCH_3$, $P\mathit{C}H_2CH_2CH_2Si$, 5 CH_2 of C_6H_{11}), 10.1–12.0 (m; $PCH_2CH_2\mathit{C}H_2Si$); MS (FD): *m/z* (%): 810 (14) [$M^+ - H$], 352 (38) [$C_{15}H_{33}O_5PSi^+$], 231 (100) [$C_{12}H_{24}O_2P^+$]; $C_{30}H_{66}ClO_8P_2RhSi_2$ (811.3): calcd C 44.41, H 8.20, Cl 4.37; found C 44.87, H 8.47, Cl 4.48.

Chlorobis[cyclohexyl(2-methoxyethyl)(3-(trimethylsilyl)propyl)phosphine-*P;O′,P′*]rhodium(I) (2b): The reaction of **1b** (173 mg, 0.6 mmol) with $[\{\mu\text{-}ClRh(COE)_2\}_2]$ (72 mg, 0.15 mmol) gave **2b** in a quantitative yield. The product was characterized by ^{31}P NMR spectroscopy. $^{31}P\{^1H\}$ NMR (32.44 MHz, acetone): δ (diastereomer I) = 57.5 (dd, $^1J(Rh,P) = 185.4$ Hz, $^2J(P,P) = 52.4$),[49] 42.7 (dd, $^1J(Rh,P) = 203.8$ Hz, $^2J(P,P) = 52.3$); δ (diastereomer II) = 57.5 (dd, $^1J(Rh,P) = 185.4$ Hz, $^2J(P,P) = 52.4$),[49] 38.9 (dd, $^1J(Rh,P) = 203.1$ Hz, $^2J(P,P) = 52.5$).

***cis/trans*-Chlorobis[cyclohexyl(2-methoxyethyl)(3-(trimethoxysilyl)propyl)-phosphine-*P*](pyridine-*N*)rhodium(I) [3a(T⁰)₂]:** Compound **2a(T⁰)₂** (153 mg, 0.19 mmol) was dissolved in CD_2Cl_2 (0.3 mL), and pyridine (0.2 mL) was added. The reaction mixture darkened to red–brown, and the resulting complex **3a(T⁰)₂** was characterized by $^{31}P\{^1H\}$ NMR spectroscopy.

***trans*-Carbonylchlorobis[cyclohexyl(2-methoxyethyl)(3-(trimethoxysilyl)propylphosphine-*P*]rhodium(I) [4a(T⁰)₂]:** A solution of **2a(T⁰)₂** (162 mg, 0.2 mmol) in acetone (4 mL) was stirred at ambient temperature under an atmosphere of CO (1 bar). The orange color of the solution turned immediately to lemon yellow. The product was purified analogously to $\mathbf{2a(T^0)_2}$ and dried under vacuum to give $\mathbf{4a(T^0)_2}$ in quantitative yield. $^{13}\mathrm{C}\{^1\mathrm{H}\}$ NMR ($\mathrm{C_6D_6}$): $\delta = 49.0$ (s; $\mathrm{SiOCH_3}$), 35.2 (vt, $N = 25.6$ Hz;[50] PCH of $\mathrm{C_6H_{11}}$), 22.1–28.3 (m; $\mathrm{P}\mathit{C}\mathrm{H_2CH_2OCH_3}$, $\mathrm{P}\mathit{C}\mathrm{H_2CH_2CH_2Si}$, 5 $\mathrm{CH_2}$ of $\mathrm{C_6H_{11}}$), 17.8 (s; $\mathrm{PCH_2}\mathit{C}\mathrm{H_2CH_2Si}$), 10.6 (vt, $N = 12.1$ Hz;[50] $\mathrm{PCH_2CH_2}\mathit{C}\mathrm{H_2Si}$); IR (acetone): $\tilde{\nu} = 1955\ \mathrm{cm^{-1}}$ ($\mathrm{C{\equiv}O}$); MS (FD): *m/z* (%): 839 (100) [M^+], 804 (25) [$M^+ - \mathrm{Cl}$], $\mathrm{C_{31}H_{66}ClO_9P_2RhSi_2}$ (839.3): calcd C 44.36, H 7.93, Cl 4.22; found C 44.57, H 7.85, Cl 4.37.

(Carbondisulfide-*C*,*S*)chlorobis[cyclohexyl(2-methoxyethyl)(3-(trimethoxysilyl)propylphosphine-*P*]rhodium(I) [$\mathbf{5a(T^0)_2}$]: A solution of $\mathbf{2a(T^0)_2}$ (153 mg, 0.19 mmol) in acetone (4 mL) was treated with carbon disulfide (0.1 mL) at 243 K. Instantaneously, the orange color of the reaction mixture darkened. The product was purified in analogy to $\mathbf{2a(T^0)_2}$ and dried under vacuum to give $\mathbf{5a(T^0)_2}$ as an orange-brown oil in quantitative yield. $^{31}\mathrm{P}\{^1\mathrm{H}\}$ NMR (101.25 MHz, [$\mathrm{D_8}$]toluene): δ (diastereomer II) = 13.0 (d, $^1J(\mathrm{Rh,P}) = 106.4$ Hz), δ (diastereomer III) = 12.9 (d, $^1J(\mathrm{Rh,P}) = 106.5$ Hz), δ (diastereomer IV) = 12.6 (d, $^1J(\mathrm{Rh,P}) = 106.5$ Hz); $^{13}\mathrm{C}\{^1\mathrm{H}\}$ NMR ([$\mathrm{D_8}$]toluene): $\delta = 50.3$ (s; $\mathrm{SiOCH_3}$), 35.2–36.0 (m; PCH of $\mathrm{C_6H_{11}}$), 19.0–29.9 (m; $\mathrm{P}\mathit{C}\mathrm{H_2CH_2OCH_3}$, $\mathrm{P}\mathit{C}\mathrm{H_2CH_2CH_2Si}$, 5 $\mathrm{CH_2}$ of $\mathrm{C_6H_{11}}$), 17.3–17.6 (m; $\mathrm{PCH_2}\mathit{C}\mathrm{H_2CH_2Si}$), 11.6–12.3 (m; $\mathrm{PCH_2CH_2}\mathit{C}\mathrm{H_2Si}$); IR (KBr): $\tilde{\nu} = 1239$ [$\nu_{\mathrm{as}}(\mathrm{CS_2})$], 1188 [$\nu_{\mathrm{s}}(\mathrm{CS_2})$], 603 $\mathrm{cm^{-1}}$ [$\delta(\mathrm{CS_2})$]; MS (FD): *m/z* (%): 854 (100) [$M^+ - \mathrm{S} - \mathrm{H}$], 819 (10) [$M^+ - \mathrm{S} - \mathrm{H} - \mathrm{Cl}$], $\mathrm{C_{31}H_{66}ClO_8P_2RhS_2Si_2}$ (887.5): calcd C 41.96, H 7.51, Cl 4.00, S: 7.23; found C 41.71, H 7.61, Cl 4.00, S 7.30.

Chlorobis[cyclohexyl(2-methoxyethyl)(3-(trimethoxysilyl)propylphosphine-*P*]-dihydrido(pyridine-*N*)rhodium(III) [$\mathbf{6a(T^0)_2}$]: A solution of $\mathbf{2a(T^0)_2}$ (167 mg, 0.21 mmol) in ethanol (5 mL) and pyridine (0.2 mL) was stirred at ambient temperature under a pressure of 1 bar hydrogen until a yellow solution was obtained. The reaction took approximately 30 min. After purification of the product $\mathbf{6a(T^0)_2}$ in analogy to $\mathbf{2a(T^0)_2}$ a light yellow oil was obtained in quantitative yield. $^{13}\mathrm{C}\{^1\mathrm{H}\}$ NMR ($\mathrm{C_6D_6}$): $\delta = 50.3$ (s; $\mathrm{SiOCH_3}$), 36.2 (vt, $N = 25.0$ Hz;[50] PCH of $\mathrm{C_6H_{11}}$), 24.8–27.9 (m; $\mathrm{P}\mathit{C}\mathrm{H_2CH_2OCH_3}$, $\mathrm{P}\mathit{C}\mathrm{H_2CH_2CH_2Si}$, 5 $\mathrm{CH_2}$ of $\mathrm{C_6H_{11}}$), 17.7 (s; $\mathrm{PCH_2}\mathit{C}\mathrm{H_2CH_2Si}$), 11.7 (s; $\mathrm{PCH_2CH_2}\mathit{C}\mathrm{H_2Si}$); $^1\mathrm{H}$ NMR ($\mathrm{C_6D_6}$): $\delta = 9.3$ (br s; *o*-H of pyridine), 6.93–7.09 (m; *p*-H of pyridine), 6.75–6.80 (m; *m*-H of pyridine), −19.1 to −18.4 (m; $\mathrm{RhH_2}$). IR (KBr): $\tilde{\nu} = 2052\ \mathrm{cm^{-1}}$ (br, $\mathrm{RhH_2}$); MS (FD): *m/z* (%): 810 (100) [$M^+ - \mathrm{pyridine} - 3\mathrm{H}$], 775 (72) [$M^+ - \mathrm{pyridine} - 3\mathrm{H} - \mathrm{Cl}$], $\mathrm{C_{35}H_{73}ClNO_8P_2RhSi_2}$ (892.5): calcd C 47.11, H 8.24, Cl 3.97, N 1.57; found C 45.95,[51] H 8.24, Cl 4.03, N 1.81.

Chlorobis[cyclohexyl(2-methoxyethyl)(3-(trimethoxysilyl)propylphosphine-*P*]-(η^2-ethene)rhodium(I) [$\mathbf{7a(T^0)_2}$]: A solution of $\mathbf{2a(T^0)_2}$ (206 mg, 0.25 mmol) in $\mathrm{C_6D_6}$ (0.5 mL) was stirred at ambient temperature under an atmosphere of ethene (1 bar). The solution immediately turned from orange to yellow. The compound $\mathbf{7a(T^0)_2}$ is only stable in the presence of ethene. $^{13}\mathrm{C}\{^1\mathrm{H}\}$ NMR ($\mathrm{C_6D_6}$): $\delta = 50.3$ (s; $\mathrm{SiOCH_3}$), 36.3 (vt, $N = 24.0$ Hz;[50] PCH of $\mathrm{C_6H_{11}}$), 19.4–30.0 (m; $\mathrm{P}\mathit{C}\mathrm{H_2CH_2OCH_3}$, $\mathrm{P}\mathit{C}\mathrm{H_2CH_2CH_2Si}$, 5 $\mathrm{CH_2}$ of $\mathrm{C_6H_{11}}$), 18.7 (s; $\mathrm{PCH_2}\mathit{C}\mathrm{H_2CH_2Si}$), 11.9 (s; $\mathrm{PCH_2CH_2}\mathit{C}\mathrm{H_2Si}$); $^1\mathrm{H}$ NMR ($\mathrm{C_6D_6}$): $\delta = 2.6$ (br s; $\mathrm{Rh(C_2H_4)}$).

Chlorobis[cyclohexyl(2-methoxyethyl)(3-(trimethoxysilyl)propylphosphine-*P*]-(η^2-diphenylacetylene)rhodium(I) [$\mathbf{8a(T^0)_2}$]: Addition of diphenylacetylene (34 mg, 0.19 mmol) to a solution of $\mathbf{2a(T^0)_2}$ (153 mg, 0.19 mmol) in *n*-hexane (6 mL) gave a yellow solution. The product was purified in analogy to $\mathbf{2a(T^0)_2}$ and dried under vacuum to give $\mathbf{8a(T^0)_2}$ as a bright yellow oil in quantitative yield. $^{31}\mathrm{P}\{^1\mathrm{H}\}$ NMR (101.25 MHz, $\mathrm{CD_2Cl_2}$): δ (diastereomer II) = 13.1 (d, $^1J(\mathrm{Rh,P}) = 115.4$ Hz); $^{13}\mathrm{C}\{^1\mathrm{H}\}$ NMR ($\mathrm{CD_2Cl_2}$): $\delta = 127$–130.7 (m; C-Ph), 69.4 (s; $\mathrm{PCH_2}\mathit{C}\mathrm{H_2OCH_3}$ of diastereomer II), 58.2 (s; $\mathrm{PCH_2CH_2O}\mathit{C}\mathrm{H_3}$ of diastereomer II), 50.6 (s; $\mathrm{SiOCH_3}$), 34.8 (vt, $N = 22.2$ Hz;[50] PCH of diastereomer I), 34.7 (vt, $N = 22.2$ Hz;[50] PCH of diastereomer II), 21.3–29.5 (m; $\mathrm{P}\mathit{C}\mathrm{H_2CH_2OCH_3}$, $\mathrm{P}\mathit{C}\mathrm{H_2CH_2CH_2Si}$, 5 $\mathrm{CH_2}$ of $\mathrm{C_6H_{11}}$), 18.9 (s; $\mathrm{PCH_2}\mathit{C}\mathrm{H_2CH_2Si}$ of diastereomer I), 18.8 (s; $\mathrm{PCH_2}\mathit{C}\mathrm{H_2CH_2Si}$ of diastereomer II), 12.0 (vt, $N = 11.5$ Hz;[50] $\mathrm{PCH_2CH_2}\mathit{C}\mathrm{H_2Si}$); IR ($\mathrm{CH_2Cl_2}$): $\tilde{\nu} = 1875\ \mathrm{cm^{-1}}$ ($\mathrm{C{\equiv}C}$); MS (FD): *m/z* (%): 989 (100) [M^+], $\mathrm{C_{44}H_{76}ClO_8P_2RhSi_2}$ (989.6): calcd C 53.41, H 7.74, Cl 3.58; found C 53.49, H 7.94, Cl 4.01.

μ-Dichloro-*trans*-bis[cyclohexyl(2-methoxyethyl)(3-(trimethoxysilyl)propylphosphine-*P*](dihydrido)rhodium(III)-*cis*-bis[cyclohexyl(2-methoxyethyl)-(3-(trimethoxysilyl)propylphosphine-*P*]rhodium(I) [$\mathbf{9a(T^0)_4}$]: A solution of $\mathbf{2a(T^0)_2}$ (143 mg, 0.18 mmol) in [$\mathrm{D_8}$]toluene (0.5 mL) was stirred at ambient temperature under an atmosphere of hydrogen (1 bar) until a yellow solution was obtained. The reaction took about 20 min. The compound $\mathbf{9a(T^0)_4}$ was only stable under an atmosphere of hydrogen. $^{31}\mathrm{P}\{^1\mathrm{H}\}$ NMR (101.25 MHz, [$\mathrm{D_8}$]toluene): δ (diastereomer II) = 34.8 (d; $^1J(\mathrm{Rh,P}) = 190.8$ Hz), δ (diastereomer II) = 28.7 (d; $^1J(\mathrm{Rh,P}) = 110.9$ Hz), δ (diastereomer III) = 28.3 (d; $^1J(\mathrm{Rh,P}) = 111.3$ Hz); $^{13}\mathrm{C}\{^1\mathrm{H}\}$ NMR ([$\mathrm{D_8}$]toluene): $\delta = 70.2$–71.2 (m; $\mathrm{PCH_2}\mathit{C}\mathrm{H_2OCH_3}$), 58.2 (s; $\mathrm{PCH_2CH_2O}\mathit{C}\mathrm{H_3}$), 50.3 (s; $\mathrm{SiOCH_3}$), 36.6 (m; PCH), 19.5–29.6 (m; $\mathrm{P}\mathit{C}\mathrm{H_2CH_2OCH_3}$, $\mathrm{P}\mathit{C}\mathrm{H_2CH_2CH_2Si}$, 5 $\mathrm{CH_2}$ of $\mathrm{C_6H_{11}}$), 18.8 (s; $\mathrm{PCH_2}\mathit{C}\mathrm{H_2CH_2Si}$), 11.8–12.5 (m; $\mathrm{PCH_2CH_2}\mathit{C}\mathrm{H_2Si}$); $^1\mathrm{H}$ NMR ([$\mathrm{D_8}$]toluene): $\delta = -21.3$ to −21.6 (m; $\mathrm{RhH_2}$); IR ($\mathrm{CH_2Cl_2}$): $\tilde{\nu} = 2065\ \mathrm{cm^{-1}}$ (br; $\mathrm{RhH_2}$).

Sol–Gel Processing: The monomeric complex $\mathbf{2(T^0)_2}$ was dissolved in the specified amount of pyridine. The solution darkened rapidly to red-brown indicating the formation of $\mathbf{3(T^0)_2}$. Subsequently *y* equiv of $\mathbf{D^0\text{-}C_6\text{-}D^0}$ ($y = 2$, 8), 2.5 times the stoichiometric amount of water, a minimum amount of MeOH, and the catalyst $(n\mathrm{Bu})_2\mathrm{Sn(OAc)_2}$ were added. The homogeneous mixtures were sealed in a Schlenk tube and stirred for approximately 14 h at ambient temperature until a swollen gel was formed. The solvent was then removed under reduced pressure, and the gels were dried for 5 h. Solvent processing was performed by stirring the large gel particles vigorously in toluene (40 mL, 12 h) to form swollen gels. The wet gels were washed with additional toluene (40 mL), EtOH (40 mL), and *n*-hexane (40 mL), and dried under vacuum (2 h).

Chlorobis[cyclohexyl(2-methoxyethyl)(3-(polysiloxanyl)propyl)phosphine-*P*;*O′*,*P′*]rhodium(I)$\mathbf{(D^i\text{-}C_6\text{-}D^i)_2}$ [$\mathbf{2(T^n)_2(D^i\text{-}C_6\text{-}D^i)_2}$]: A mixture of $[\mathrm{ClRh}(\overset{\frown}{\mathrm{PO}})(\mathrm{P{\sim}O})]$ [$\mathbf{2a(T^0)_2}$] (394 mg, 0.49 mmol), 2 equiv of $\mathbf{D^0\text{-}C_6\text{-}D^0}$ (286 mg, 0.97 mmol), pyridine (0.4 mL), MeOH (1 mL), water (153 mg, 8.51 mmol), and $(n\mathrm{Bu})_2\mathrm{Sn(OAc)_2}$ (34 mg, 0.10 mmol) was processed by sol–gel methods to yield 518 mg (98 %) of $\mathbf{2(T^n)_2(D^i\text{-}C_6\text{-}D^i)_2}$ as an orange gel. $^{31}\mathrm{P}$ CP/MAS NMR (dynamic parameters [$\nu_{\mathrm{rf}} = 7.5$ kHz]): $\delta = 57.9$ ($T_{\mathrm{PH}} = 0.21$ ms, $T_{1\rho\mathrm{H}} = 10.3$ ms), 42.5 ($T_{\mathrm{PH}} = 0.19$ ms, $T_{1\rho\mathrm{H}} = 10.3$ ms) 57.9 ($T_{\mathrm{PH}} = 0.16$ ms, $T_{1\rho\mathrm{H}} = 10.3$ ms); $^{13}\mathrm{C}$ CP/MAS NMR: $\delta = 49.7$ ($\mathrm{SiOCH_3}$), 38–23.4 ($\mathrm{C_6H_{11}}$, $\mathrm{Si(CH_2)_2}\mathit{C}\mathrm{H_2}\mathit{C}\mathrm{H_2(CH_2)_2Si}$, $\mathrm{P}\mathit{C}\mathrm{H_2}\mathit{C}\mathrm{H_2CH_2Si}$, $\mathrm{P}\mathit{C}\mathrm{H_2CH_2OCH_3}$), 17.9 ($\mathrm{PCH_2CH_2}\mathit{C}\mathrm{H_2Si}$, $\mathrm{Si(}\mathit{C}\mathrm{H_2)_2CH_2CH_2(}\mathit{C}\mathrm{H_2)_2Si}$), −0.2 ($\mathrm{SiCH_3}$); $^{29}\mathrm{Si}$ CP/MAS NMR (silicon substructure): $\delta = -2.3$ ($\mathrm{D^0}$, $I_0 = 2.9$), −14.6 ($\mathrm{D^1}$, $I_0 = 33.0$), −22.1 ($\mathrm{D^2}$, $I_0 = 123.9$), −55.5 ($\mathrm{T^1}$, $I_0 = 3.1$), −59.9 ($\mathrm{T^2}$, $I_0 = 24.6$), −67.6 ($\mathrm{T^3}$, $I_0 = 37.8$), real T:D ratio = 1:2.4, degree of condensation of the D groups = 88 %, degree of condensation of the T groups = 84 %;[52] $\mathrm{N_2}$ surface area: $1.6\ \mathrm{m^2\,g^{-1}}$; $\mathrm{C_{40}H_{84}ClO_9P_2RhSi_6}$ (idealized stoichiometry): calcd C 44.57, H 7.85, Cl 3.71; corrected stoichiometry:[53] C 44.02, H 7.99, Cl 3.01; found C 42.77, H 8.30, Cl 3.71.

Chlorobis[cyclohexyl(2-methoxyethyl)(3-(polysiloxanyl)propyl)phosphine-*P*;*O′*,*P′*]rhodium(I)$\mathbf{(D^i\text{-}C_6\text{-}D^i)_8}$ [$\mathbf{2(T^n)_2(D^i\text{-}C_6\text{-}D^i)_8}$]: A mixture of $[\mathrm{ClRh}(\overset{\frown}{\mathrm{PO}})(\mathrm{P{\sim}O})]$ [$\mathbf{2(T^0)_2}$] (219 mg, 0.27 mmol), 8 equiv of $\mathbf{D^0\text{-}C_6\text{-}D^0}$ (637 mg, 2.16 mmol), pyridine (0.2 mL), MeOH (1 mL), water (231 mg, 12.85 mmol), and $(n\mathrm{Bu})_2\mathrm{Sn(OAc)_2}$ (34 mg, 0.10 mmol) was processed by sol–gel methods to yield 613 mg (99 %) of $\mathbf{2(T^n)_2(D^i\text{-}C_6\text{-}D^i)_8}$ as an orange gel. $^{13}\mathrm{C}$ CP/MAS NMR: $\delta = 49.7$ ($\mathrm{SiOCH_3}$), 38–23.4 ($\mathrm{C_6H_{11}}$, $\mathrm{Si(CH_2)_2}\mathit{C}\mathrm{H_2}\mathit{C}\mathrm{H_2(CH_2)_2Si}$, $\mathrm{P}\mathit{C}\mathrm{H_2}\mathit{C}\mathrm{H_2CH_2Si}$, $\mathrm{P}\mathit{C}\mathrm{H_2CH_2OCH_3}$), 17.9 ($\mathrm{PCH_2CH_2}\mathit{C}\mathrm{H_2Si}$, $\mathrm{Si(}\mathit{C}\mathrm{H_2)_2CH_2CH_2(}\mathit{C}\mathrm{H_2)_2Si}$), −0.1 ($\mathrm{SiCH_3}$); $^{29}\mathrm{Si}$ CP/MAS NMR (silicon substructure): $\delta = -2.1$ ($\mathrm{D^0}$, $I_0 = 8.7$), −13.8 ($\mathrm{D^1}$, $I_0 = 15.4$), −22.4 ($\mathrm{D^2}$, $I_0 = 78.6$), −58.8 ($\mathrm{T^2}$, $I_0 = 6.2$), −67.6 ($\mathrm{T^3}$, $I_0 = 7.4$), real T:D ratio = 1:7.6, degree of condensation of the D groups = 84 %, degree of condensation of the T groups = 85 %;[52] $\mathrm{N_2}$ surface area: 0.9 $\mathrm{m^2/g}$; $\mathrm{C_{88}H_{192}ClO_{21}P_2RhSi_{18}}$ (idealized stoichiometry): calcd C 46.11, H 8.44, Cl 1.55; corrected stoichiometry:[53] C 45.00, H 8.49, Cl 1.57; found C 44.16, H 8.72, Cl 1.59.

***trans*-Carbonylchlorobis[cyclohexyl(2-methoxyethyl)(3-(polysiloxanylpropyl)-phosphine-*P*]rhodium(I)$\mathbf{(D^i\text{-}C_6\text{-}D^i)_2}$** [$\mathbf{4(T^n)_2(D^i\text{-}C_6\text{-}D^i)_2}$]: A Schlenk tube was charged with the powdery gel $\mathbf{2(T^n)_2(D^i\text{-}C_6\text{-}D^i)_2}$ (226 mg, 0.21 mmol), which was exposed to an atmosphere of carbon monoxide (1 bar) and stirred with a magnetic stirring bar. The color rapidly changed to lemon yellow. After evaporation under vacuum the product $\mathbf{4(T^n)_2(D^i\text{-}C_6\text{-}D^i)_2}$ was obtained quantitatively. $^{13}\mathrm{C}$ CP/MAS NMR: $\delta = 49.8$ ($\mathrm{SiOCH_3}$), 38–23.4 ($\mathrm{C_6H_{11}}$, $\mathrm{Si(CH_2)_2}\mathit{C}\mathrm{H_2}\mathit{C}\mathrm{H_2(CH_2)_2Si}$, $\mathrm{P}\mathit{C}\mathrm{H_2}\mathit{C}\mathrm{H_2CH_2Si}$, $\mathrm{P}\mathit{C}\mathrm{H_2CH_2OCH_3}$), 17.7 ($\mathrm{PCH_2CH_2}\mathit{C}\mathrm{H_2Si}$, $\mathrm{Si(}\mathit{C}\mathrm{H_2)_2CH_2CH_2(}\mathit{C}\mathrm{H_2)_2Si}$), −0.2 ($\mathrm{SiCH_3}$); IR (KBr): $\delta = 1952\ \mathrm{cm^{-1}}$ ($\mathrm{C{\equiv}O}$); $\mathrm{C_{41}H_{84}ClO_{10}P_2RhSi_6}$ (idealized stoichiometry): calcd C 44.53, H 7.66, Cl 3.21; corrected stoichiometry:[53] C 43.99, H 7.80, Cl 2.94; found C 43.24, H 7.93, Cl 2.88.

0947-6539/97/0311-1843 $ 17.50+.50/0

(Carbondisulfide-*C*,*S*)chlorobis[cyclohexyl(2-methoxyethyl)(3-(polysiloxanylpropyl)phosphine-*P*]rhodium(I)$(\mathbf{D}^i\text{-}\mathbf{C}_6\text{-}\mathbf{D}^i)_2$ [5$(\mathbf{T}^n)_2(\mathbf{D}^i\text{-}\mathbf{C}_6\text{-}\mathbf{D}^i)_2$]: Upon addition of CS_2 (0.2 mL) to a suspension of **2**$(\mathbf{T}^n)_2(\mathbf{D}^i\text{-}\mathbf{C}_6\text{-}\mathbf{D}^i)_2$ (200 mg, 0.19 mmol) in *n*-hexane (20 mL) at 243 K, the color rapidly darkened. The orange-brown polymer was washed with *n*-hexane (20 mL) and dried under vacuum to give **5**$(\mathbf{T}^n)_2(\mathbf{D}^i\text{-}\mathbf{C}_6\text{-}\mathbf{D}^i)_2$ in a quantitative yield. ^{13}C CP/MAS NMR: $\delta = 49.9$ ($SiOCH_3$), 38–23.3 (C_6H_{11}, $Si(CH_2)_2\mathit{C}H_2\mathit{C}H_2(CH_2)_2Si$, $P\mathit{C}H_2\mathit{C}H_2CH_2Si$, $P\mathit{C}H_2CH_2OCH_3$), 17.5 ($PCH_2CH_2\mathit{C}H_2Si$, $Si(\mathit{C}H_2)_2$-$CH_2CH_2(\mathit{C}H_2)_2Si$), −0.4 ($SiCH_3$); IR (KBr): $\tilde{\nu} = 1242$ [$\nu_{as}(CS_2)$], 1193 [$\nu_s(CS_2)$], 605 cm^{-1} [$\delta(CS_2)$]; $C_{41}H_{84}ClO_9P_2RhS_2Si_6$ (idealized stoichiometry): calcd C 42.67, H 7.34, Cl 3.07, S 5.56; corrected stoichiometry:[53] C 42.31, H 7.50, Cl 2.83, S 5.11; found C 42.46, H 7.53, Cl 3.10, S 6.03.

Chlorobis[cyclohexyl(2-methoxyethyl)(3-(polysiloxanylpropyl)phosphine-*P*]-dihydrido(pyridine-*N*)rhodium(III)$(\mathbf{D}^i\text{-}\mathbf{C}_6\text{-}\mathbf{D}^i)_2$ [6$(\mathbf{T}^n)_2(\mathbf{D}^i\text{-}\mathbf{C}_6\text{-}\mathbf{D}^i)_2$]: A suspension of **2**$(\mathbf{T}^n)_2(\mathbf{D}^i\text{-}\mathbf{C}_6\text{-}\mathbf{D}^i)_2$ (163 mg, 0.15 mmol) in a mixture of EtOH (10 mL) and pyridine (0.5 mL) was exposed to an atmosphere of hydrogen (1 bar). The reaction mixture was stirred for about 30 min. The product was washed with toluene (20 mL) and *n*-hexane (20 mL). After evaporation under vacuum 142 mg (81%) of **6**$(\mathbf{T}^n)_2(\mathbf{D}^i\text{-}\mathbf{C}_6\text{-}\mathbf{D}^i)_2$ was obtained as a light yellow powder. ^{13}C CP/MAS NMR: $\delta = 49.7$ ($SiOCH_3$), 38–23.4 (C_6H_{11}, $Si(CH_2)_2\mathit{C}H_2\mathit{C}H_2(CH_2)_2Si$, $P\mathit{C}H_2\mathit{C}H_2CH_2Si$, $P\mathit{C}H_2CH_2OCH_3$), 18.2 ($PCH_2CH_2\mathit{C}H_2Si$, $Si(\mathit{C}H_2)_2CH_2CH_2(\mathit{C}H_2)_2Si$), −0.3 ($SiCH_3$); IR (KBr): $\tilde{\nu} = 2056\ cm^{-1}$ (br; RhH_2); $C_{45}H_{91}ClNO_9P_2RhSi_6$ (idealized stoichiometry): calcd C 46.63, H 7.91, Cl 3.06, N 1.21; corrected stoichiometry:[53] C 45.95, H 8.03, Cl 2.81, N 1.11; found C 44.68, H 7.92, Cl 3.09, N 0.82.

Chlorobis[cyclohexyl(2-methoxyethyl)(3-(polysiloxanylpropyl)phosphine-*P*]-(η^2-ethene)]rhodium(I)$(\mathbf{D}^i\text{-}\mathbf{C}_6\text{-}\mathbf{D}^i)_2$ [7$(\mathbf{T}^n)_2(\mathbf{D}^i\text{-}\mathbf{C}_6\text{-}\mathbf{D}^i)_2$]: A Schlenk tube was charged with the powdery gel **2**$(\mathbf{T}^n)_2(\mathbf{D}^i\text{-}\mathbf{C}_6\text{-}\mathbf{D}^i)_2$ (100 mg, 0.09 mmol), which was exposed to an atmosphere of ethene (1 bar) and stirred with a magnetic stirring bar. The color rapidly changed to yellow. After 30 min the yellow polymer **7**$(\mathbf{T}^n)_2(\mathbf{D}^i\text{-}\mathbf{C}_6\text{-}\mathbf{D}^i)_2$ was directly transferred into a zirconia rotor and characterized by solid state NMR spectroscopy. ^{13}C CP/MAS NMR: $\delta = 49.8$ ($SiOCH_3$), 38–23.4 (C_6H_{11}, $Si(CH_2)_2\mathit{C}H_2\mathit{C}H_2(CH_2)_2Si$, $P\mathit{C}H_2\mathit{C}H_2CH_2Si$, $P\mathit{C}H_2CH_2OCH_3$), 17.7 ($PCH_2CH_2\mathit{C}H_2Si$, $Si(\mathit{C}H_2)_2$-$CH_2CH_2(\mathit{C}H_2)_2Si$), −0.2 ($SiCH_3$).

Chlorobis[cyclohexyl(2-methoxyethyl)(3-(polysiloxanylpropyl)phosphine-*P*]-(η^2-diphenylacetylene)rhodium(I)$(\mathbf{D}^i\text{-}\mathbf{C}_6\text{-}\mathbf{D}^i)_2$ [8$(\mathbf{T}^n)_2(\mathbf{D}^i\text{-}\mathbf{C}_6\text{-}\mathbf{D}^i)_2$]: The starting complex **2**$(\mathbf{T}^n)_2(\mathbf{D}^i\text{-}\mathbf{C}_6\text{-}\mathbf{D}^i)_2$ (183 mg, 0.17 mmol) was allowed to swell in toluene (5 mL). After 10 min a solution of tolan (151 mg, 0.85 mmol) in toluene (5 mL) was added, and the reaction mixture was stirred for 30 min. The supernatant solution was separated, and the solid washed with toluene (10 mL) and *n*-hexane (20 mL). The product was dried under vacuum to yield 187 mg (88%) of **8**$(\mathbf{T}^n)_2(\mathbf{D}^i\text{-}\mathbf{C}_6\text{-}\mathbf{D}^i)_2$ as an intensive yellow gel. ^{13}C CP/MAS NMR: $\delta = 49.7$ ($SiOCH_3$), 38–23.5 (C_6H_{11}, $Si(CH_2)_2\mathit{C}H_2\mathit{C}H_2(CH_2)_2Si$, $P\mathit{C}H_2\mathit{C}H_2CH_2Si$, $P\mathit{C}H_2CH_2OCH_3$), 17.7 ($PCH_2CH_2\mathit{C}H_2Si$, $Si(\mathit{C}H_2)_2$-$CH_2CH_2(\mathit{C}H_2)_2Si$), −0.2 ($SiCH_3$); IR (KBr): $\tilde{\nu} = 1870\ cm^{-1}$ ($C\equiv C$); $C_{54}H_{94}ClO_9P_2RhSi_6$ (idealized stoichiometry): calcd C 51.63, H 7.54, Cl 2.82; corrected stoichiometry:[53] C 49.15, H 7.75, Cl 2.70; found C 46.46, H 7.73, Cl 2.78.

Oxidative Addition of Hydrogen to 2$(\mathbf{T}^n)_2(\mathbf{D}^i\text{-}\mathbf{C}_6\text{-}\mathbf{D}^i)_2$: A Schlenk tube was charged with the powdery gel **2**$(\mathbf{T}^n)_2(\mathbf{D}^i\text{-}\mathbf{C}_6\text{-}\mathbf{D}^i)_2$ (150 mg, 0.14 mmol), which was exposed to an atmosphere of hydrogen (1 bar) and stirred with a magnetic stirring bar. The color rapidly changed to yellow. After 30 min the product was directly transferred into a zirconia rotor and investigated by ^{31}P CP/MAS NMR and then IR spectroscopy.

Behavior of 2b under Sol–Gel Conditions: A solution of **2b** (87 mg, 0.12 mmol) in MeOH (1 mL) was treated with water (16 mg, 0.9 mmol), pyridine (0.4 mL), and $(nBu)_2Sn(OAc)_2$ (34 mg, 0.10 mmol). The red-brown mixture was stirred for 14 h. After evaporation of the volatiles **2b** was recovered, as shown by $^{31}P\{^1H\}$ NMR spectroscopy.

Acknowledgment: The support of this research by the Deutsche Forschungsgemeinschaft (Forschergruppe, grant no. Li 154/41-3), Bonn/Bad Godesberg, and by the Fonds der Chemischen Industrie, Frankfurt/Main, is gratefully acknowledged. We are grateful to Degussa, Germany, for a generous gift of $RhCl_3 \cdot H_2O$ and to Wacker Chemie for a generous gift of $HSi(Me)Cl_2$. We thank Prof. K. G. Nickel, Institut für Mineralogie, University of Tübingen, and Dipl.-Chem. W. Wielandt, Institut für Anorganische Chemie, University of Tübingen, for BET measurements.

Received: January 28, 1997 [F 587]
Revised version: June 9, 1997

---

[1] F. R. Hartley, *Supported Metal Complexes*, D. Reidel, Dordrecht, **1985**.
[2] U. Deschler, P. Kleinschmit, P. Panster, *Angew. Chem.* **1986**, *98*, 237; *Angew. Chem. Int. Ed. Engl.* **1986**, *25*, 236.
[3] C. J. Brinker, G. W. Scherer, *Sol Gel Science*, Academic Press, London, **1990**.
[4] E. Lindner, M. Kemmler, H. A. Mayer, P. Wegner, *J. Am. Chem. Soc.* **1994**, *116*, 348.
[5] D. A. Loy, K. J. Shea, *Chem. Rev.* **1995**, *95*, 1431 and references therein.
[6] R. J. P. Corriu, J. J. E. Moreau, P. Thepot, M. Wong Chi Man, C. Choro, J.-P. Lère-Porte, J.-L. Sauvajol, *Chem. Mater.* **1994**, *6*, 640.
[7] D. A. Loy, G. M. Jamison, B. M. Baugher, S. A. Myers, R. A. Assink, K. J. Shea, *Chem. Mater.* **1996**, *8*, 656.
[8] R. Corriu, D. Leclercq, *Angew. Chem.* **1996**, *108*, 1524; *Angew. Chem. Int. Ed. Engl.* **1996**, *35*, 1420.
[9] Fn–T/Q, Fn–T/T, Fn–T/D, and Fn–T/D-C_z-D blends represent copolymers prepared by co-condensation of Fn–$Si(OMe)_3$ (Fn–T) with $Si(OEt)_4$ ($\mathbf{Q}^0$), $MeSi(OMe)_3$ ($\mathbf{T}^0$), $Me_2Si(OEt)_2$ ($\mathbf{D}^0$), and $MeSi(OMe)_2(CH_2)_z(MeO)_2SiMe$ ($\mathbf{D}^0\text{-}\mathbf{C}_z\text{-}\mathbf{D}^0$), respectively. Fn (functionality) = $PhP(CH_2CH_2OMe)(CH_2)_x$-, [*cis*-Cl(H)Ru(CO)]$_{1/3}$$P(Ph)(CH_2CH_2OMe)(CH_2)_x$-, $[Cl_2Pd]_{1/2}P(Ph)$-$(CH_2CH_2OMe)(CH_2)_3$-, and [*trans*-ClRh(CO)]$_{1/2}$$P(Ph)(CH_2CH_2OMe)$-$(CH_2)_3$-, respectively.
[10] E. Lindner, T. Schneller, H. A. Mayer, H. Bertagnolli, T. S. Ertel, W. Hörner, *Chem. Mater.* **1997**, *9*, 1524.
[11] E. Lindner, R. Schreiber, T. Schneller, P. Wegner, H. A. Mayer, W. Göpel, C. Ziegler, *Inorg. Chem.* **1996**, *35*, 514.
[12] E. Lindner, M. Kemmler, T. Schneller, H. A. Mayer, *Inorg. Chem.* **1995**, *34*, 5489.
[13] D. W. Sindorf, G. E. Maciel, *J. Am. Chem. Soc.* **1983**, *105*, 3767.
[14] E. Bayer, K. Albert, J. Reiners, M. Nieder, D. Müller, *J. Chromatogr.* **1983**, *264*, 197.
[15] J. Blümel, *Inorg. Chem.* **1994**, *33*, 5050.
[16] E. Lindner, R. Schreiber, M. Kemmler, T. Schneller, H. A. Mayer, *Chem. Mater.* **1995**, *7*, 951.
[17] E. Lindner, A. Jäger, T. Schneller, H. A. Mayer, *Chem. Mater.* **1997**, *9*, 81.
[18] For nomenclature, see footnote on p. 1833.
[19] E. Lindner, Q. Wang, H. A. Mayer, A. Bader, *J. Organomet. Chem.* **1993**, *458*, 229.
[20] E. Lindner, S. Meyer, P. Wegner, B. Karle, A. Sickinger, B. Steger, *J. Organomet. Chem.* **1987**, *335*, 59.
[21] E. Lindner, A. Bader, E. Glaser, B. Pfleiderer, W. Schumann, E. Bayer, *J. Organomet. Chem.* **1988**, *355*, 45.
[22] E. Lindner, W. Wielandt, unpublished results.
[23] A. Bader, E. Lindner, *Coord. Chem. Rev.* **1991**, *108*, 27.
[24] H. Werner, A. Hampp, K. Peters, E. M. Peters, L. Walz H. G. Schnering, *Z. Naturforsch.* **1990**, *45b*, 1548.
[25] E. Lindner, Q. Wang, H. A. Mayer, A. Bader, H. Kühbauch, P. Wegner, *Organometallics* **1993**, *12*, 3291.
[26] P. E. Garrou, *Chem. Rev.* **1981**, *81*, 229.
[27] E. Lindner, R. Fawzi, H. A. Mayer, K. Eichele, W. Hiller, *Organometallics* **1992**, *11*, 1033.
[28] E. Lindner, B. Keppeler, H. A. Mayer, K. Gierling, R. Fawzi, M. Steimann, *J. Organomet. Chem.* **1996**, *526*, 175.
[29] Owing to the chirality of the ether–phosphine ligands **1a**$(\mathbf{T}^0)$ and **1b**, all their rhodium complexes exist in diastereomeric forms. However, only in some cases (**2a**$(\mathbf{T}^0)_2$, **2b**, **5a**$(\mathbf{T}^0)_2$, **8a**$(\mathbf{T}^0)_2$, **9a**$(\mathbf{T}^0)_4$) are the signals of different diastereomeric forms resolved in the $^{31}P\{^1H\}$ NMR spectra.
[30] C. Bianchini, D. Masi, C. Mealli, A. Meli, M. Sabat, *Organometallics* **1985**, *4*, 1014.
[31] S. B. Duckett, C. L. Newell, R. Eisenberg, *J. Am. Chem. Soc.* **1994**, *116*, 10548.
[32] C. A. Tolman, P. Z. Meakin, D. L. Lindner, J. P. Jesson, *J. Am. Chem. Soc.* **1974**, *96*, 2762.
[33] B. T. Heaton, J. A. Iggo, C. Jacob, J. Nadaraiah, M. A. Fontaine, R. Messere, A. F. Noels, *J. Chem. Soc. Dalton Trans.* **1994**, 2875.
[34] P. Binger, J. Haas, G. Glaser, R. Goddard, C. Krüger, *Chem. Ber.* **1994**, *127*, 1927.
[35] H. Werner, A. Hampp, B. Windmüller, *J. Organomet. Chem.* **1992**, *435*, 169.
[36] H. L. M. van Gaal, F. L. A. van den Bekerom, *J. Organomet. Chem.* **1977**, *134*, 237.
[37] H. Werner, R. Feser, *Z. Naturforsch.* **1980**, *35b*, 689.
[38] a) The accuracy of quantitative CP/MAS NMR spectroscopy is generally estimated to be around ±10%; b) K. J. Shea, D. A. Loy, O. Webster, *J. Am. Chem. Soc.* **1992**, *114*, 6700; c) M. Mehring, *Principles of High Resolution NMR in Solids*, 2nd ed., Springer, Berlin, **1983**.
[39] The overall degree of hydrolysis of the D and T species in the Fn–T/D-C_z-D copolymers is calculated by the following equation: $100[(3T+2D) - A($Si-

$OCH_3)/A(CH_2\text{-}O\text{-}CH_3)]/(3T+2D)$; T = real amount of T species in the polymer; D = real amount of D species in the polymer; $A(Si\text{-}OCH_3)$ = peak area of the nonhydrolyzed Si-O-CH_3 group in the ^{13}C CP/MAS NMR spectrum; $A(CH_2\text{-}O\text{-}CH_3)$ = peak area of the methoxy group in the ^{13}C CP/MAS NMR spectrum.

[40] J. M. Brown, A. G. Kent, *J. Chem. Soc. Perkin Trans. II* **1987**, 1597.

[41] J. Halpern, T. Okamoto, A. Zakhariev, *J. Mol. Catal.* **1976**, *2*, 65.

[42] R. H. Grubbs, C. Gibbons, L. C. Kroll, W. D. Bonds, C. H. Brubaker, *J. Am. Chem. Soc.* **1973**, *95*, 2373.

[43] K. Kochloefl, W. Liebelt, H. Knözinger, *J. Chem. Soc. Chem. Commun.* **1977**, 510.

[44] J. P. Collman, *Acc. Chem. Res.* **1968**, *1*, 136.

[45] J. Schaefer, E. O. Stejskal, R. Buchdahl, *Macromolecules* **1977**, *10*, 384.

[46] R. K. Harris, *Analyst* **1985**, *110*, 649.

[47] R. Voelkel, *Angew. Chem.* **1988**, *100*, 1525; *Angew. Chem. Int. Ed. Engl.* **1988**, *27*, 1468.

[48] A. van der Ent, A. L. Onderdelinden, *Inorg. Synth.* **1973**, *14*, 92.

[49] At this field strength only the signals of the two diastereomers in the high field region of the $^{31}P\{^1H\}$ NMR spectrum were resolved.

[50] a) $N = |^1J_{PC} + {}^3J_{PC}|$; b) R. K. Harris, *Can. J. Chem.* **1964**, *42*, 2275.

[51] a) Although high temperatures and V_2O_5 (catalyst) were used for C, H analyses, the carbon values remained low. This is probably due to incomplete combustion, which may be caused by rhodium; b) T. E. Nappier Jr., D. W. Meek, R. M. Kirchner, J. A. Ibers, *J. Am. Chem. Soc.* **1973**, *95*, 4194.

[52] The degree of condensation of the T species: $100(T^1 + 2T^2 + 3T^3)/[3(T^1 + T^2 + T^3)]$, degree of condensation of the D species: $100(D^1 + 2D^2)/[2(D^0 + D^1 + D^2)]$; T^1, T^2, T^3, D^0, D^1, D^2 are the relative amounts of silyl species present in the sample.

[53] The corrected stoichiometry was obtained by adding the additional number of OH units of the D^0, D^1, D^2, T^1, T^2, and T^3 groups (obtained from the ^{29}Si CP/MAS NMR spectra) to the idealized stoichiometry (only D^2 and T^3 units). The real T:D ratio and the degree of hydrolysis were also taken into account.

0947-6539/97/0311-1845 $ 17.50+.50/0